AD-A153 243 PROPERTIES OF DEFECTS IN HG1-XCDXTE(U) ROCKWELL INTERNATIONAL THOUSAND OAKS CA SCIENCE CENTER S H SHIN ET AL. NOV 84 SC5305.6FR ARO-17721.7EL 1/1

UNCLASSIFIED DAAG29-81-C-0012 F/G 20/2 NL

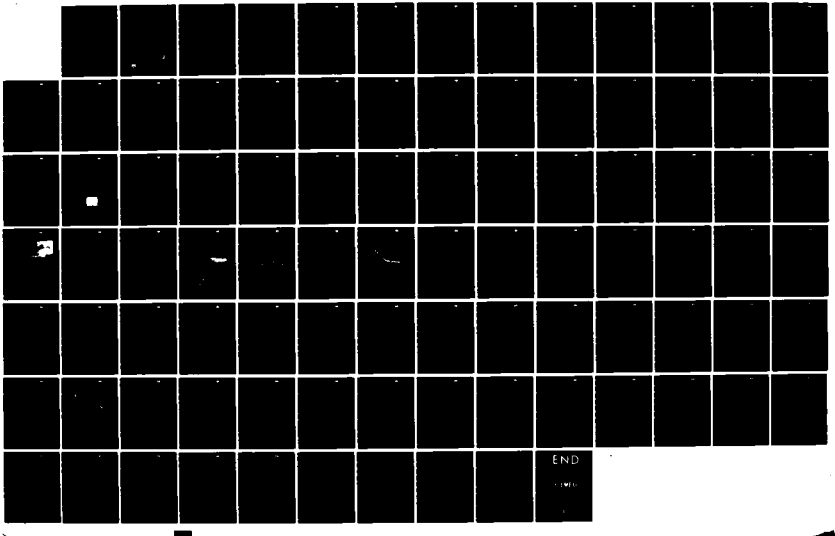

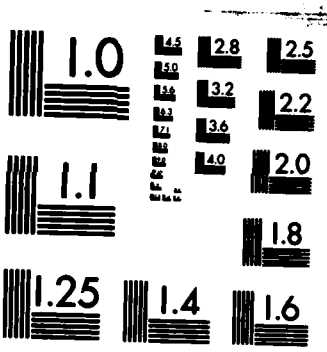

SC5305.6FR

Copy No. 38

PROPERTIES OF DEFECTS IN $Hg_{1-x}Cd_xTe$

FINAL TECHNICAL REPORT FOR THE PERIOD
July 1, 1981 through September 30, 1984

S.H. Shin and J. Bajaj
Principal Investigators

NOVEMBER 1984

Prepared for

U.S. Army Research Office
P.O. Box 12211
Research Triangle Park, NC 27709

CONTRACT NO. DAAG29-81-C-0012
PROJECT NO. 1L161102BH57-03 ELECTRONICS

Rockwell International Science Center
1049 Camino Dos Rios
Thousand Oaks, CA 91360

Rockwell International
Science Center

UNCLASSIFIED
SECURITY CLASSIFICATION OF THIS PAGE

AD-A153 243

REPORT DOCUMENTATION PAGE

1a. REPORT SECURITY CLASSIFICATION Unclassified	1b. RESTRICTIVE MARKINGS
2a. SECURITY CLASSIFICATION AUTHORITY	3. DISTRIBUTION/AVAILABILITY OF REPORT Approved for public release; distribution unlimited.
2b. DECLASSIFICATION/DOWNGRADING SCHEDULE	
4. PERFORMING ORGANIZATION REPORT NUMBER(S) SC5305.6FR	5. MONITORING ORGANIZATION REPORT NUMBER(S)
6a. NAME OF PERFORMING ORGANIZATION Rockwell International Science Center 6b. OFFICE SYMBOL (If applicable)	7a. NAME OF MONITORING ORGANIZATION
6c. ADDRESS (City, State and ZIP Code) 1049 Camino Dos Rios Thousand Oaks, CA 91360	7b. ADDRESS (City, State and ZIP Code)
8a. NAME OF FUNDING/SPONSORING ORGANIZATION U.S. Army Research Office 8b. OFFICE SYMBOL (If applicable)	9. PROCUREMENT INSTRUMENT IDENTIFICATION NUMBER Contract No. DAAG29-81-C-0021
8c. ADDRESS (City, State and ZIP Code) Post Office Box 12211 Research Triangle Park, NC 27709	10. SOURCE OF FUNDING NOS PROGRAM ELEMENT NO. / PROJECT NO. 1L161102-BH57-03 Electronics / TASK NO / WORK UNIT NO.
11. TITLE (Include Security Classification) PROPERTIES OF DEFECTS IN $Hg_{1-x}Cd_xTe$ (U)	
12. PERSONAL AUTHOR(S) Shin, Soo H.; Bajaj, Jagmohan	
13a. TYPE OF REPORT Final Technical Report 13b. TIME COVERED FROM 07/01/81 TO 09/30/84	14. DATE OF REPORT (Yr., Mo., Day) NOVEMBER 1984 15. PAGE COUNT 84

16. SUPPLEMENTARY NOTATION
The view, opinions, and/or findings contained in this report are those of the authors and should not be construed as an official Department of the Army position, policy, or decision, unless so designated by other documentation.

17 COSATI CODES		
FIELD	GROUP	SUB GR

18. SUBJECT TERMS (Continue on reverse if necessary and identify by block number)
LPE HgCdTe, defects, cation vacancy, minority carrier lifetime Te precipitates, annealing, TEM, Auger Spectroscopy, X-ray diffraction, Raman scattering, photoluminescence, admittance spectroscopy, DLTS, acceptor ionization energies, double acceptors.

19. ABSTRACT (Continue on reverse if necessary and identify by block number)

This final report covers the progress made over the July 1, 1981 through September 30, 1984 period, The majority of the contract effort was focused in this period on systematic investigations of the basic physics of defects in HgCdTe.

Detailed electrical characterization of LPE HgCdTe has been carried out. The normal range of values in carrier concentrations, mobilities and minority carrier lifetimes was established by Hall effect and photoconductive decay lifetime measurements. The total equilibrium concentration of cation vacancies was studied qualitatively and compared with model calculations. The results show that the doubly ionized vacancy state is dominant and the cation vacancy formation energy (E_f) is found to be 0.9 $\pm$ 0.1 eV for $Hg_{1-x}Cd_xTe$ and nearly independent of the Cd composition x.

Te precipitates in CdTe have been characterized by Auger spectroscopy, x-ray diffraction and Raman spectroscopy. The x-ray results show that the precipitated Te in Bridgman-grown CdTe crystals has the same structural phase as observed in elemental Te under high pressure. Auger and Raman microprobe spectroscopy—

20. DISTRIBUTION/AVAILABILITY OF ABSTRACT	21. ABSTRACT SECURITY CLASSIFICATION
UNCLASSIFIED/UNLIMITED ☒ SAME AS RPT. ☐ DTIC USERS ☐	Unclassified
22a. NAME OF RESPONSIBLE INDIVIDUAL	22b. TELEPHONE NUMBER (Include Area Code) / 22c. OFFICE SYMBOL

DD FORM 1473, 83 APR EDITION OF 1 JAN 73 IS OBSOLETE.

UNCLASSIFIED
SECURITY CLASSIFICATION OF THIS PAGE

(Block 19 Continued)

were carried out to confirm Te precipitates in CdTe and identify the symmetry of the Te precipitates.

Acceptor ionization energies (E_A) in $Hg_{1-x}Cd_xTe$ material were also investigated as a function of annealing temperature. These E_A values, as observed from Hall measurements, decrease from 20 to 10 meV as anneal temperature decreases from 488 to 347°C.

The interaction of rare gas Xe and He atoms in HgCdTe has been investigated using Xe or He/Hg mixtures for ambient during the anneal. This study results in consistently lower carrier concentrations and higher mobilities for p-type LWIR HgCdTe. Rare gas interaction with Hg vacancies is believed to be responsible for the observed improvements.

Photoluminescence (PL) measurements carried out on SWIR large gap LPE $Hg_{1-x}Cd_xTe$ and its CdTe substrate indicate that the same neutral donor may be present in both materials, whereas the impurity or defect responsible for one PL line in CdTe is undetectable in LPE $Hg_{1-x}Cd_xTe$ epitaxial layers.

Far infrared absorption spectra of Cu in CdTe are found to exhibit a characteristic broad feature with a pronounced fine structure. Several sets of sharp transitions are separated by 21.2 meV which corresponds to the LO phonon, and each set has vibrational side bands with spacing equal to the TA phonon (3.6 meV).

Admittance spectroscopy studies on MWIR p-HgCdTe ($x \simeq 0.31$) samples show two majority carrier traps at 13 and 40 meV in sample 3-524 and two traps at 23 and 70 meV in sample 4-31. The level at 13 meV has been previously observed in both bulk and LPE HgCdTe. The other three levels have not been reported. Possible candidates for such defects are substitutional C_{Te} and Si_{Te} both of which are expected to be double acceptors and which often occur as impurities.

In summary we have carried out experimental studies on the vacancies and defects in the LPE $Hg_{1-x}Cd_xTe$ alloy system. These results provide better understanding of the problems associated with CdTe substrates and LPE $Hg_{1-x}Cd_xTe$ epilayers.

TABLE OF CONTENTS

LIST OF ILLUSTRATIONS

LIST OF ILLUSTRATIONS

LIST OF ILLUSTRATIONS

LIST OF TABLES

FOREWORD

This final report covers results carried out under the "Properties of Defects in $Hg_{1-x}Cd_xTe$" program for the period from July 1, 1981 to September 30, 1984. This report was prepared by the Rockwell International Science Center, Thousand Oaks, California under Contract No. DAAG29-81-C-0012. The Contract Monitor was Dr. H.R. Wittmann of U.S. Army Research Office at Research Triangle Park.

The principal investigator for this program was Dr. S.H. Shin. The principal technical support for this work at the Science Center was provided by Dr. J. Bajaj. The program manager was Dr. D.T. Cheung.

The authors would like to express their appreciation to Drs. M. Khoshnevisan and W.E. Tennant for their encouragement and very helpful discussions, and to Dr. K. Elliot (MRDC) for admittance study and Prof. B.J. Feldman of University of Missouri for photoluminescence measurements on HgCdTe, and Drs. C. Morgan-Pond and R. Raghavan for theoretical calculations of the p-type carrier concentrations in HgCdTe.

We are grateful to Drs. J.E. Huffmann and M.G. Stapelbroek for their help in far infrared measurements, and Mr. G.L. Bostrup and D.D. Edwall for providing some of the samples, and Mr. J.G. Pasko for photoconductor fabrication, Ms. L. Bubulac for SIMS analysis, and Mr. R.V. Gil for CdTe sample preparation.

Helpful discussions with Prof. D.S. Pan of UCLA and Dr. C.B. Norris of Sandia Lab are gratefully acknowledged. Thanks are also due to Mr. J. Murray and J. Madden of the Youth Motivation Program for help in some of the Hall measurements.

1.0 INTRODUCTION AND SUMMARY

1.1 Introduction

Mercury Cadmium Telluride ($Hg_{1-x}Cd_xTe$) photodetectors are currently the Army's choice for infrared systems in both the 3-5 μm and 8-12 μm spectral windows. During recent years, technical progress in HgCdTe, particularly in photovoltaic devices, has been very rapid and impressive; however, most of the research and development efforts have been focused on devices designed for specific system applications. There has been a general lack of fundamental research on the basic properties of HgCdTe itself. A thorough understanding of the fundamental properties is critical not only to improved device performance and reliability but may also lead to new applications of this important alloy semiconductor system.

One of the most important needs in the fundamental study of HgCdTe is the understanding of the equilibrium concentrations of native defects in HgCdTe. Unlike group IV or III-V compounds, the electrical properties of p-type HgCdTe are believed to be dominated by cation vacancies. The physics of defect formation and the electrical properties and stabilities of such defects are currently poorly understood, yet this information is of utmost importance in the practical applications of HgCdTe detectors. Therefore, this research effort was undertaken on HgCdTe epitaxial layers under support from Army Research Office in which experimental measurements of the cation vacancy formation energies of HgCdTe were performed. Comparisons were made with the theoretical calculations of the p-type carrier concentrations in $Hg_{0.8}Cd_{0.2}Te$ by Morgan-Pond and R. Raghavan which are in good agreement with the experimental data. This final report details the results of experimental efforts to study the defect-related physical properties of the LPE HgCdTe alloy system.

1.2 Summary

This report consists of ten sections. In Section 2.0 we present the transport properties of LPE HgCdTe material. These include electron

mobility and minority carrier lifetime in n-type $Hg_{1-x}Cd_xTe$. In Section 3.0 equilibrium cation vacancy concentrations related to p-type conduction in LPE $Hg_{1-x}Cd_xTe$ are described. The discussions represent fundamental considerations that needed to be addressed in the course of the program. Section 4.0 describes the nature of Te precipitates in CdTe and impurity gettering at the LPE HgCdTe/ CdTe interface. The substitution of the rare gases Xe and He in Hg vacancies has been studied in $Hg_{1-x}Cd_xTe$, and a tentative interpretation of anomalous electrical properties are described in Section 5.0. Photoluminescence studies of LPE HgCdTe and its CdTe substrate and far infrared absorption spectroscopy of CdTe are described in Sections 6.0 and 7.0, and admittance studies of $Hg_{0.7}Cd_{0.3}Te$ are discussed in Section 8.0. Sections 9.0 and 10.0 include the summary and references, respectively. Appendix I contains electrical properties of as-grown LPE HgCdTe.

1.3 Publications

The following presentations and publications have resulted from the work performed throughout the period of this program.

1. J. Bajaj, S.H. Shin, G. Bostrup and D.T. Cheung, "Electron Mobility in LPE $Hg_{1-x}Cd_xTe$/CdTe Layers Near Zero Bandgap Crossing," J. Vac. Sci. Technol. 21(1), 244 (1982).

2. S.H. Shin, J. Bajaj and D.T. Cheung, "Characterization of LPE $Hg_{1-x}Cd_xTe$," Proc. The IRIS Detector Specialty Group Meeting, San Diego, 1982.

3. S.H. Shin, J. Bajaj, L.A. Moudy and D.T. Cheung, "Characterization of Te Precipitates in CdTe Crystals," Appl. Phys. Lett. 43(1), 68 (1983).

4. J. Bajaj, S.H. Shin, J.G. Pasko and M. Khoshnevisan, "Minority Carrier Lifetime in LPE $Hg_{1-x}Cd_xTe$," J. Vac. Sci. Technol. A 1(3), 1749 (1983).

5. B.J. Feldman, J. Bajaj and S.H. Shin, "Photoluminescence in Liquid Phase Epitaxially Grown $Hg_{0.3}Cd_{0.7}Te$," J. Appl. Phys. 55(10), 3873 (1984).

6. B.J. Feldman, J. Bajaj and S.H. Shin, "Photoluminescence in Liquid Phase Epitaxially Grown $Hg_{0.3}Cd_{0.7}Te$ and its CdTe Substrate at 4.2K and 77K," International Conference on Luminescence, Madison, Wisconsin (1984) to be published in J. Lum. (1985).

7. S.H. Shin, M. Khoshnevisan, C. Morgan-Pond and R. Raghavan, "Cation Vacancy Formation Energies in LPE $Hg_{1-x}Cd_xTe$," submitted to Appl. Phys. Lett.

8. S.H. Shin, G.L. Bostrup and M. Khoshnevisan, "Equilibrium of Noble Gases Xe and He with $Hg_{0.79}Cd_{0.21}Te$," in preparation.

2.0 TRANSPORT PROPERTIES OF LPE $Hg_{1-x}Cd_xTe$/CdTe

In recent years, considerable attention has been focused on the fundamental physics and chemistry of HgCdTe, particularly liquid phase epitaxial (LPE)-grown HgCdTe. Although advanced devices such as the hybrid focal plane arrays and MIS charge coupled devices have been successfully demonstrated in LPE-grown HgCdTe material, the current HgCdTe technology is still not optimized. It is apparent that some key material parameters that affect the ultimate device performance are not yet fully identified and controlled. In particular the physics of defect formation and the electrical properties are poorly understood, yet this information is of utmost importance in developing HgCdTe detector technology. Therefore, extensive research on the HgCdTe system is being conducted at many technology centers including a few university laboratories.

Liquid phase epitaxy layers of $Hg_{1-x}Cd_xTe$ ($0.16 < x < 0.75$) grown on CdTe (111) substrates have been characterized. Before conducting measurements to study the properties of defects in LPE HgCdTe, the normal range of values for carrier density, mobility and lifetimes in both p- and n-type HgCdTe epilayers was established by Hall effect and excess carrier lifetime measurements. The results are comparable to those reported for bulk n- and p-type material. This work results of Hall effect and minority carrier lifetime measurements on HgCdTe epitaxial layers are presented.

$Hg_{1-x}Cd_xTe$ layers were grown by a liquid phase epitaxial technique (LPE) on undoped CdTe substrates.[1] The thickness of the LPE layer was typically 15-30 μm. The samples were converted to n-type by annealing in a Hg atmosphere at 210°C for about 5 h. For Hall measurements, samples were cut in rectangular shapes, with typical dimensions 8 × 4 mm^2 and then etched in 1% Br-methanol for 10 s. Indium and gold metal contacts were made for ohmic contacts to n-type and p-type $Hg_{1-x}Cd_xTe$, respectively. Samples were mounted in a variable temperature dewar using GE varnish and the Hall measurements were carried out by the standard Van der Pauw method.

The composition x for each sample was determined by electron microprobe analysis. Depth profile of x shows that the composition is uniform except within 1-2 μm near the $Hg_{1-x}Cd_xTe$/CdTe interface, as shown in Fig. 1. These concentration gradients near the interface do not affect our measurements. In the Van der Pauw technique contacts are made on the surface so the layer appears as a graded resistance. Since the resistance of large x material is much larger than the resistance of small x material, only the constant x region is probed.

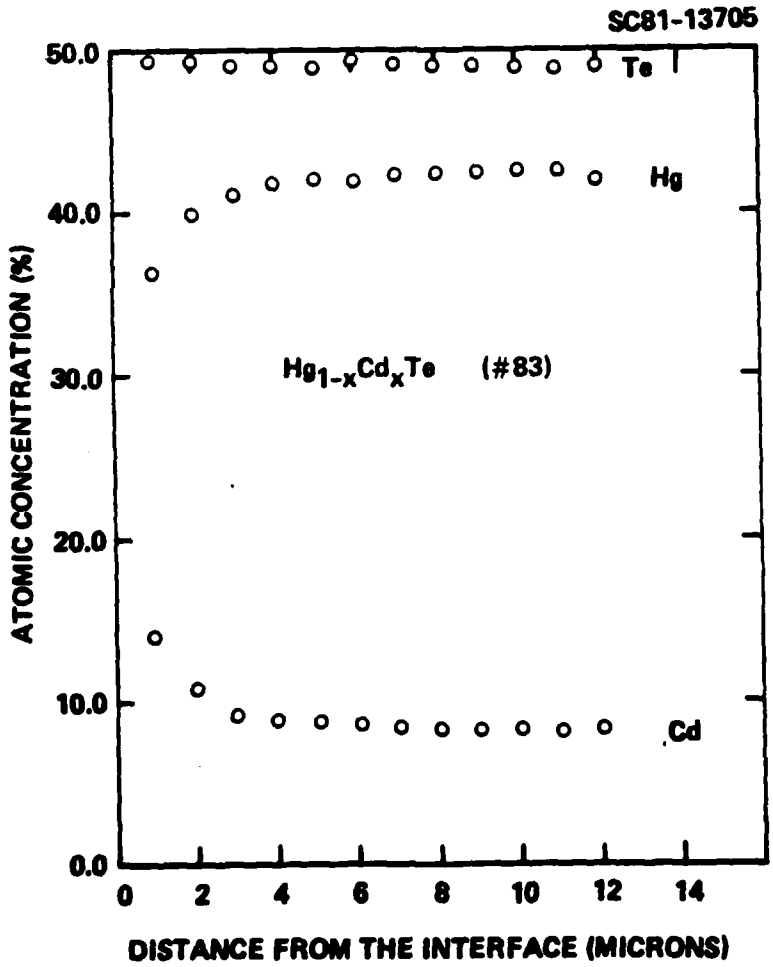

Fig. 1 Compositional depth profile of LPE HgCdTe.

2.1 As-grown $Hg_{1-x}Cd_xTe$

Table 1 lists the carrier concentrations of as-grown epilayers with different Cd composition x. At 77K, the as-grown epilayers are always p-type with a hole concentration of the order of $\sim 10^{17}$ and $\sim 10^{16}$ cm^{-3} for x = 0.2 and x = 0.3 $Hg_{1-x}Cd_xTe$ material, respectively. The epilayers grown from Te-rich solution, at ~ 500°C would be expected to have carrier concentrations of $\sim 10^{17}$ cm^{-3} for any Cd composition. Contrary to expectation, however, the carrier concentration depends on the Cd composition and varies up to two orders of magnitude in the $0.2 \leq x \leq 0.7$ range. Similarly, the measured mobilities of different composition p-type HgCdTe layers decrease as x increases. It is conceivable that since it takes about four hours for the epilayer to cool down to room temperature after the growth, the epilayers get annealed under excess Hg vapor pressure in the furnace resulting in different carrier concentrations for different Cd composition. Weakness of Hg-Te bond as compared to Cd-Te bond may also explain this variation of acceptor concentration with x. The Hg-Te bond becomes weaker as Hg concentration increases. As a consequence, Hg vacancy concentration, acting as acceptors, increases as Cd composition decreases.

Table 1

Carrier Concentration and Mobility of As-grown p-Type $Hg_{1-x}Cd_xTe$ Layers, T = 77K

x Value (λ_{co})	Carrier Conc. (cm^{-3})	Hole Mobility ($cm^2/V\text{-}s$)
x = 0.21 (10.5 μm)	1.5×10^{17}	300
x = 0.30 (5.0 μm)	1.4×10^{16}	250
x = 0.42 (2.7 μm)	7.0×10^{15}	180
x = 0.68 (1.4 μm)	10×10^{15}	110

Figure 2 shows the variation of Hall coefficient, hole mobility and resistivity with temperature for $Hg_{1-x}Cd_xTe$ with x = 0.42. It is noted that the Hall coefficient sign does not change at room temperature but remains p-type for x = 0.42 (λ_{co} = 2.7 μm) $Hg_{1-x}Cd_xTe$ sample. Further electrical properties of as-grown $Hg_{1-x}Cd_xTe$ epilayers with $0.195 < x < 0.351$ were published[2] (Appendix).

2.2 Electron Mobility in LPE $Hg_{1-x}Cd_xTe$/CdTe Layers

The electron mobility in n-type $Hg_{1-x}Cd_xTe$ has been studied as a function of temperature in the vicinity of zero bandgap crossing. The temperature range covered in these experiments was 5-300K, and the samples studied were liquid phase epitaxial $Hg_{1-x}Cd_xTe$/CdTe layers. A distinct narrow peak in the mobility μ_H observed for x = 0.16 at 40K, which we interpret as an effect related to zero bandgap crossing. The value of μ_H at the peak is 1.3×10^6 $cm^2\ V^{-1}\ s^{-1}$.

We have studied in detail the electron Hall mobility, carrier concentration and resistivity in n-type LPE $Hg_{1-x}Cd_xTe$/CdTe layers as a function of temperature. The temperature range investigated is 5-300K. We report here the Hall effect measurements on samples with Cd composition x in the range 0.12 to 0.23.

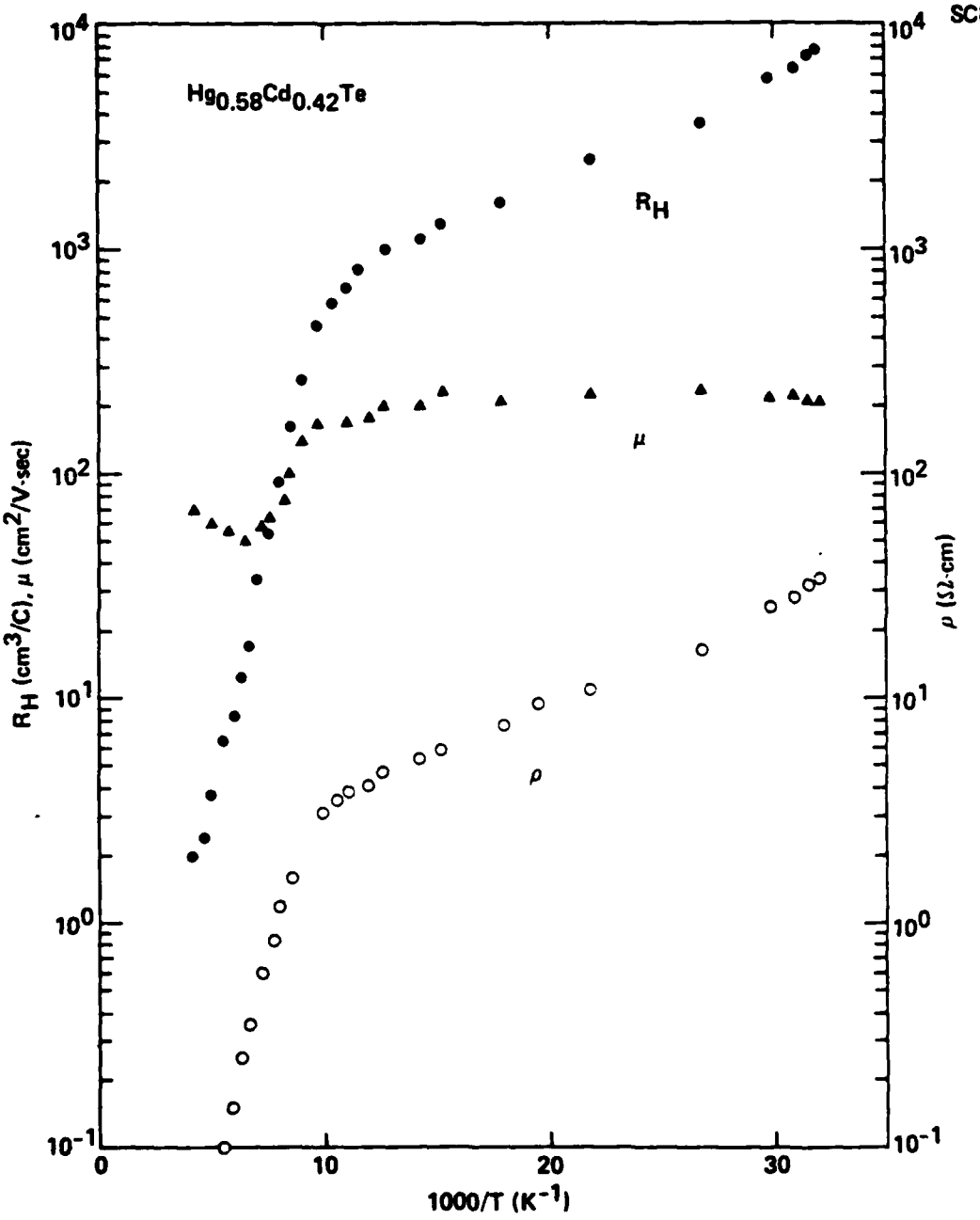

Fig. 2 Hall coefficients (R_H), hole mobility (μ) and resistivity (ρ) as a function of temperature in as-grown $Hg_{0.58}Cd_{0.42}Te$.

Figure 3 shows the variation of electron mobility, carrier concentration and resistivity with temperature for $Hg_{1-x}Cd_xTe$ with x = 0.16. The carrier concentration remains intrinsic down to about 30K. The intrinsic concentration vs T in the range 100-300K is in excellent agreement with Schmit's[3] calculations. The extrinsic carrier concentration is 4.5×10^{14} cm^{-3}. A distinct prominent peak in the mobility curve is observed at 40K; our suggestion is that it is related to zero bandgap crossing. In support of this assertion, we note that near x = 0.16 the variation of bandgap Eg with x is $\partial Eg/\partial x$ = 18.3 meV/% of Cd[4] and the variation of Eg with temperature is $\partial Eg/\partial T$ = 0.4 meV/K.[5] Assuming that the bandgap equals zero at 0 K for x = 0.165, then the bandgap for x = 0.16 should become zero at a temperature $T_{0.16} = 18.3 \times 0.5/0.4 = 23K$. This value is not very far from the experimentally determined value of 40K for $T_{0.16}$, as shown in our data.

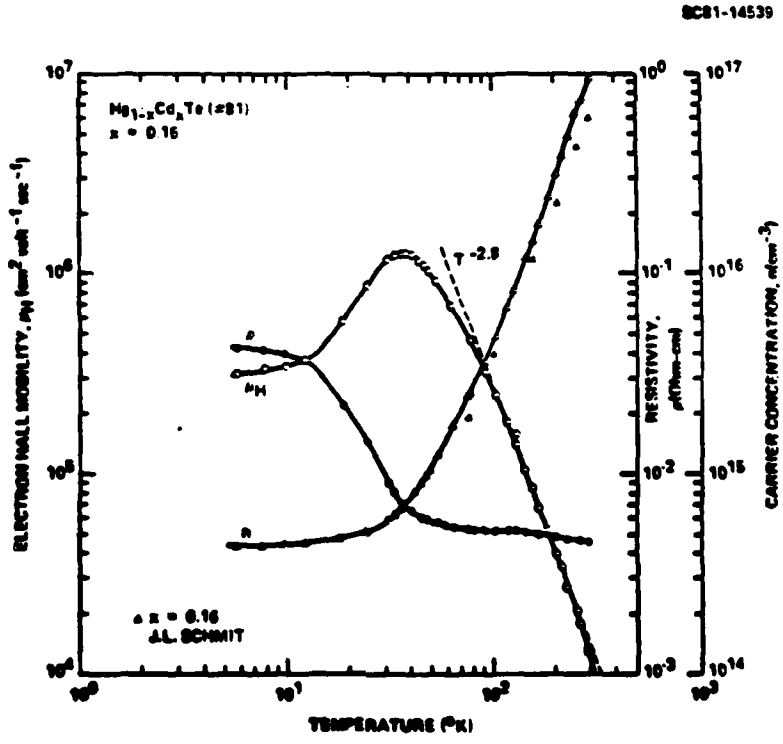

Fig. 3 Electron Hall mobility, carrier concentration, and resistivity as a function of temperature.

We also note that a peak in temperature dependence of mobility can arise due to competition between different scattering mechanisms for electrons. Since ionized impurity scattering gives a mobility temperature dependence with a positive power law and the lattice vibration scattering gives a mobility temperaure dependence with a negative power law, the joint effect of these contributions at low temperatures will produce a peak in mobility. However, the peak observed for $x = 0.16$ $Hg_{1-x}Cd_xTe$ is narrower and more distinct than that for samples with different composition x, therefore, we believe it is related to zero bandgap crossing.

To our knowledge there is no self-consistent, quantitative model for the band structure and the transport calculations in the vicinity of zero bandgap crossing. However, qualitatively a peak in the temperature dependent mobility can be expected due to an important band crossing effect involving the change in the sign of the temperature coefficient of the energy gap on either side of the zero gap crossing.[5] This band structure variation effect would be reflected in the mobility via the scattering transitions over the carrier states,

$$\mu \propto \frac{e\tau}{m^*} \quad . \tag{1}$$

For elastic scattering, expected to be the dominant scattering at low temperatures

$$\frac{1}{\tau} \propto \rho(E), \text{ the density of states} \quad . \tag{2}$$

Therefore

$$\mu \propto \frac{1}{m^* \rho(E)} \quad . \tag{3}$$

The effective mass m^* and the density of states ρ for small gaps are functions of E_g due to admixing of valence and conduction band states and tend to a minimum at zero gap. This in turn can produce a peak in the mobility.

To check the reproducibility of this peak, two other samples from different layers with the same composition were studied; both of these samples showed a similar peak around 40K. The results for all three samples are shown in Fig. 4. At higher temperatures, the mobility for each sample shows the same behavior, declining with a power law of $T^{-2.8}$. The dominant scattering mechanisms limiting the mobility in this temperature range is the scattering by optical phonons. Each sample gives a peak in mobility at nearly the same temperature and the magnitude of the mobility at the peak is identical. There is, however, a marked difference in the mobility at lower temperatures. As seen in Fig. 4, there seem to be a definite correlation between the extrinsic carrier concentration and the fall in mobility at low temperatures; the larger the extrinsic carrier concentration, the lower is the mobility. In all these measurements a magnetic field of 6 kG was used. However, the peak is observed even at lower magnetic field with the values of μ_H increasing with decreasing field.

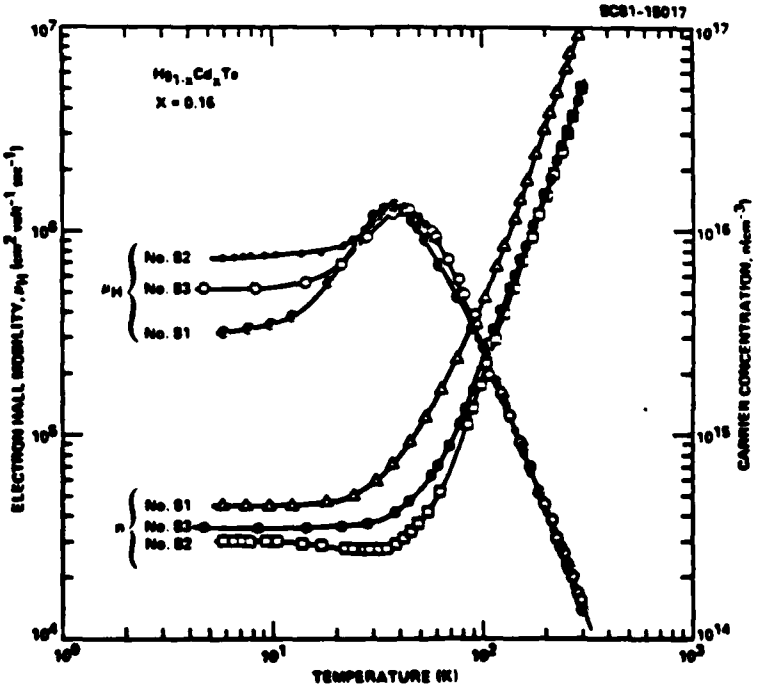

Fig. 4 Electron Hall mobility and carrier concentration as a function of temperature for three different $Hg_{0.84}Cd_{0.16}Te$ samples.

Figures 5 and 6 show the temperature dependence of Hall measurements for $Hg_{1-x}Cd_xTe$ samples with different x values as indicated. For x = 0.192 and 0.227 the behavior of μ_H with temperature is similar to results reported earlier.[6,7] For x = 0.138, the behavior of μ_H as a function of temperature is similar to the results of Dubowski et al.[8] The peak value of $\mu_H = 4 \times 10^6$ cm^2/Vs is, however, higher than that reported earlier.

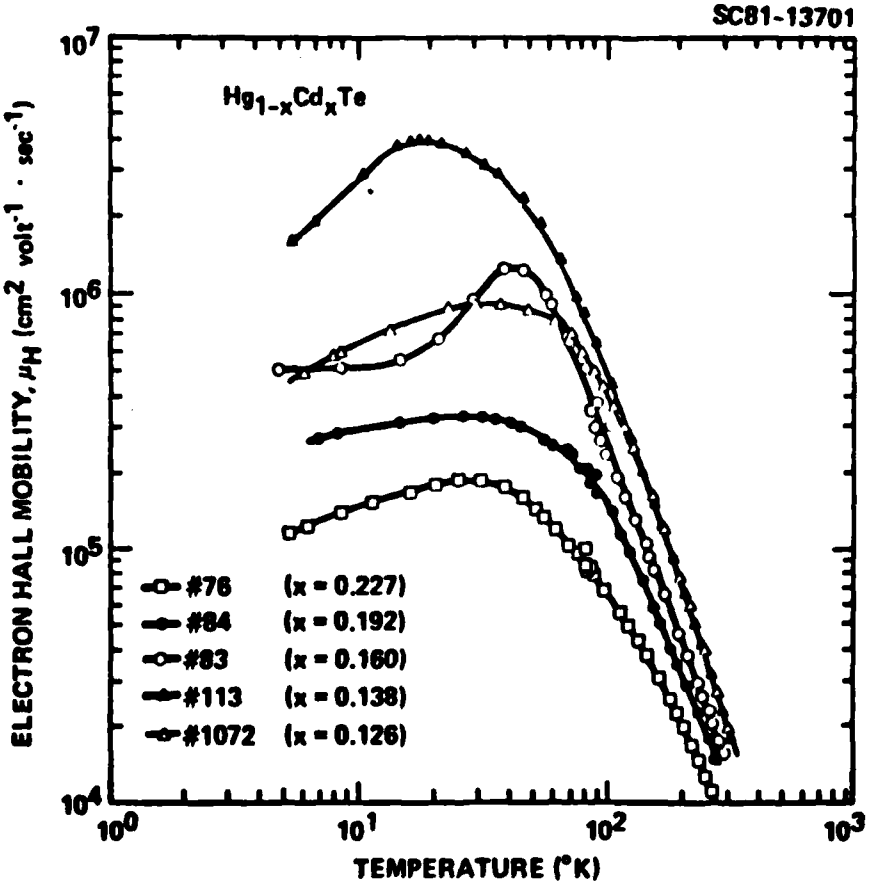

Fig. 5 Electron Hall mobility as a function of temperature for LPE HgCdTe/CdTe layers.

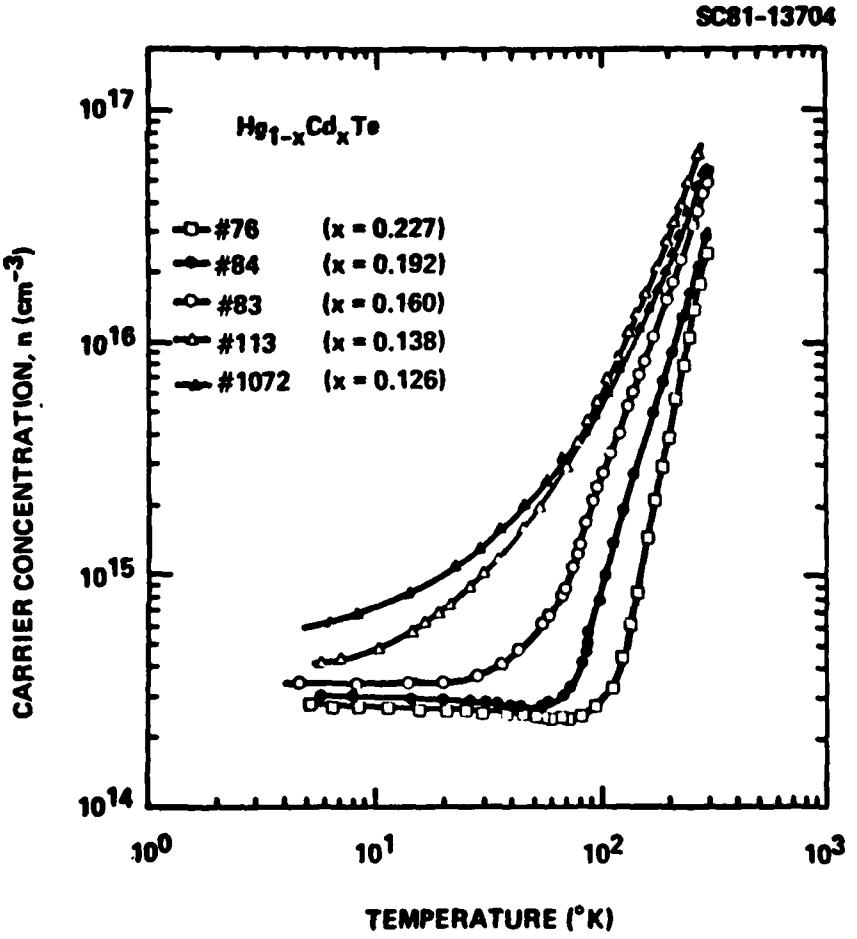

Fig. 6 Carrier concentration as a function of temperature for LPE HgCdTe/CdTe samples.

In conclusion, we have examined the electrical transport properties of LPE $Hg_{1-x}Cd_xTe$ layers near zero bandgap crossing. Our measurements show that the transport properties of LPE $Hg_{1-x}Cd_xTe$ are comparable to the best bulk $Hg_{1-x}Cd_xTe$. A distinct narrow peak in electron mobility in n-type $Hg_{0.84}Cd_{0.16}Te$ at 40K appears to be related to zero bandgap crossing. A detailed theoretical calculation of transport properties near zero bandgap

crossing is now in progress by D.S. Pan. Once these results are available, a more definite conclusion regarding the nature of the peak can be reached.

2.3 Minority Carrier Lifetime in LPE $Hg_{1-x}Cd_xTe$

We report measurements on the minority carrier lifetime in n-type and p-type LPE $Hg_{1-x}Cd_xTe$/CdTe with $x \sim 0.2$. For n-HgCdTe, we have measured lifetimes of 4-7 μs at 77K for passivated samples. These values are comparable to the results reported for bulk material. For p-HgCdTe epilayers with thickness < 20 μm, the measured lifetime is 15-20 ns at 77K and is suspected to be limited by surface recombination. With excitation through the CdTe substrate, we have attempted to measure the bulk lifetime. Preliminary results are reported.

2.3.1 Introduction

A systematic study of the minority carrier lifetime in n- and p-type liquid phase epitaxially (LPE) grown $Hg_{1-x}Cd_xTe$ ($x \sim 0.2$) has been carried out as a function of temperature. LPE HgCdTe is intrinsically different from bulk HgCdTe as it is grown from a Te-rich solution. There are also composition gradients near the interface with the substrate, and the layer thickness is comparable to the minority carrier diffusion length. These differences affect the minority carrier lifetime in LPE material. Except for a recent study on n-HgCdTe layers,[9] little work has been reported in the literature. A detailed analysis of lifetime in LPE HgCdTe was therefore undertaken.

We have also carried out a parallel theoretical analysis of lifetime limited by the three dominant recombination mechanisms: radiative, Auger, and Shockley-Read. Since parameters like the energy bandgap $E_g(T,x)$ and intrinsic carrier concentration $n_i(x,T)$ are explicitly involved in these derivations, we have examined different expressions for $E_g(x,T)$ and $n_i(x,T)$ reported in the literature and compared them with experimental data on LPE $Hg_{1-x}Cd_xTe$ layers.

2.3.2 Experimental

All samples studied were LPE $Hg_{1-x}Cd_xTe$ grown on CdTe substrates. As-grown samples are p-type. The samples were converted to n-type by annealing in a Hg atmosphere at 210°C for about 10 hours. Samples of typical dimensions 5 × 4 mm^2 were etched in Br-methanol prior to measurements. Indium and gold were used for ohmic contacts to n-type and p-type samples, respectively. After mounting in a variable temperature dewar, the samples were masked such that only the central 1 × 1 mm^2 areas of the samples were exposed.

The minority carrier lifetime was measured by a photoconductive decay technique using short (~ 20 ns) pulses from a GaAs laser. The photoconductive response was recorded on a 7854-Tektronix waveform processing oscillopscope. The stored decay trace was plotted on a semilog scale to check if the decay was exponential.

It was experimentally observed that for light intensities above certain levels, (~ 10^4 watts/cm^2), there was a non-exponential start to the decay curve. This was avoided by keeping the light intensity low. The non-exponential behavior at high intensities appears consistent with the shortening of surface lifetimes due to high carrier concentration, and is relatively independent of surface passivation.

As expected, the measured lifetimes were observed to increase with decreasing background radiation. The lifetimes reported here were measured under low background conditions achieved by placing a thin plate of Al_2O_3 in front of the samples. The Al_2O_3 plate and the sample were maintained at nearly the same temperature.

2.3.2.1 n-Type LPE $Hg_{1-x}Cd_xTe$

We have observed lifetimes of the order of 1 μs at 77K in unpassivated n-$Hg_{1-x}Cd_xTe$ (with $x \approx 0.21$). The carrier concentration (n_e) and mobility (μ_e) at 77K in these samples were typically 1.4 × 10^{14} cm^{-3} and 1.3 × 10^5 cm^2/V-s, respectively. The measured lifetime as a function of

temperature on sample N4-249 is shown in Fig. 7. The results are quite typical of the samples that were examined. To determine the value of Cd composition x, the electron concentration $n_e(T)$ was first obtained from Hall effect measurements as a function of temperature. The values of $n_e(T)$ were then compared with theoretical values calculated using the expression for $E_g(x,T)$ and $n_i(x,T)$ reported by Nemirovsky et al[10] and Hansen et al.[11] As shown in Fig. 8, our data fit very well to the theoretical values calculated by using expressions from both groups with x = 0.212. This value of x was, therefore, used to calculate the intrinsic radiative (τ_{R_i}) and Auger (τ_{A_i}) lifetimes using the expressions:[6]

$$\tau_{R_i} = \frac{1}{2Bn_i} \tag{4}$$

$$\tau_{A_i} = \frac{7.6 \times 10^{-18} \varepsilon_\infty^2 (1 + m_e/m_h)^{1/2} (1 + 2\, m_e/m_h) \exp \dfrac{(1 + 2\, m_e/m_h)\, E_g}{(1 + m_e/m_h) kT}}{\dfrac{m_e}{m_o} |F_1 F_2|^2 \left(\dfrac{kT}{E_g}\right)^{3/2}} \tag{5}$$

where

$m_o \equiv$ rest mass of the electron

$m_e \equiv$ effective mass of electrons

$m_h \equiv$ effective mass of of holes = 0.55 m_o

$\varepsilon_\infty \equiv$ high frequency dielectric constant

$F_1F_2 \equiv$ overlap integral[12] = 0.3

$B \equiv$ capture probability, as given by the following equation:[6]

$$B = 5.8 \times 10^{-13}\ \varepsilon_\infty^{1/2} \left(\frac{m_o}{m_e + m_h}\right)^{3/2} \left(1 + \frac{m_o}{m_e} + \frac{m_o}{m_h}\right) \left(\frac{300}{T}\right)^{3/2} E_g^{\,2} \tag{6}$$

For x = 0.212 the theoretical τ_{A_i} and τ_{R_i} were calculated and are shown in Fig. 7. The solid and dashed lines are obtained by using the expressions for $E_g(x,T)$ and $n_i(x,T)$ from Nemirovsky et al and Hansen et al, respectively.

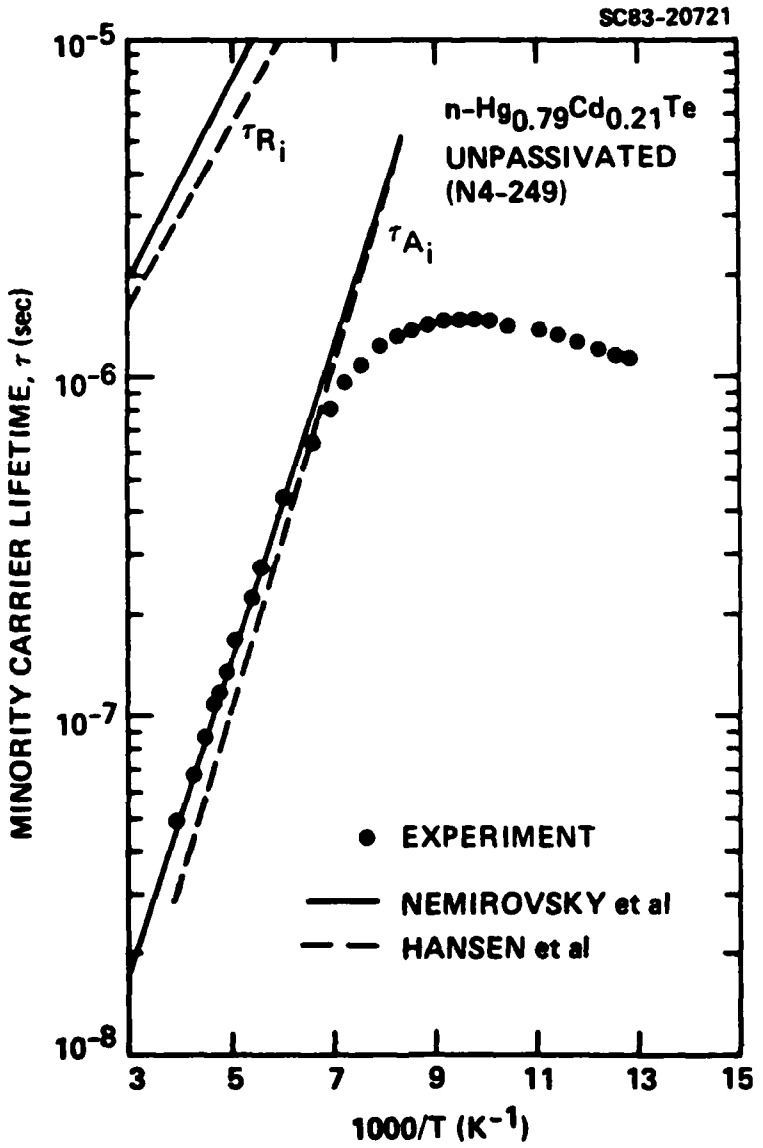

Fig. 7 Temperature dependence of minority carrier lifetime in unpassivated n-type $Hg_{0.79}Cd_{0.21}Te$. The solid and dashed lines are theoretical lifetimes calculated using the expression for $n_i(x,T)$ from Ref. 10 and Ref. 11, respectively.

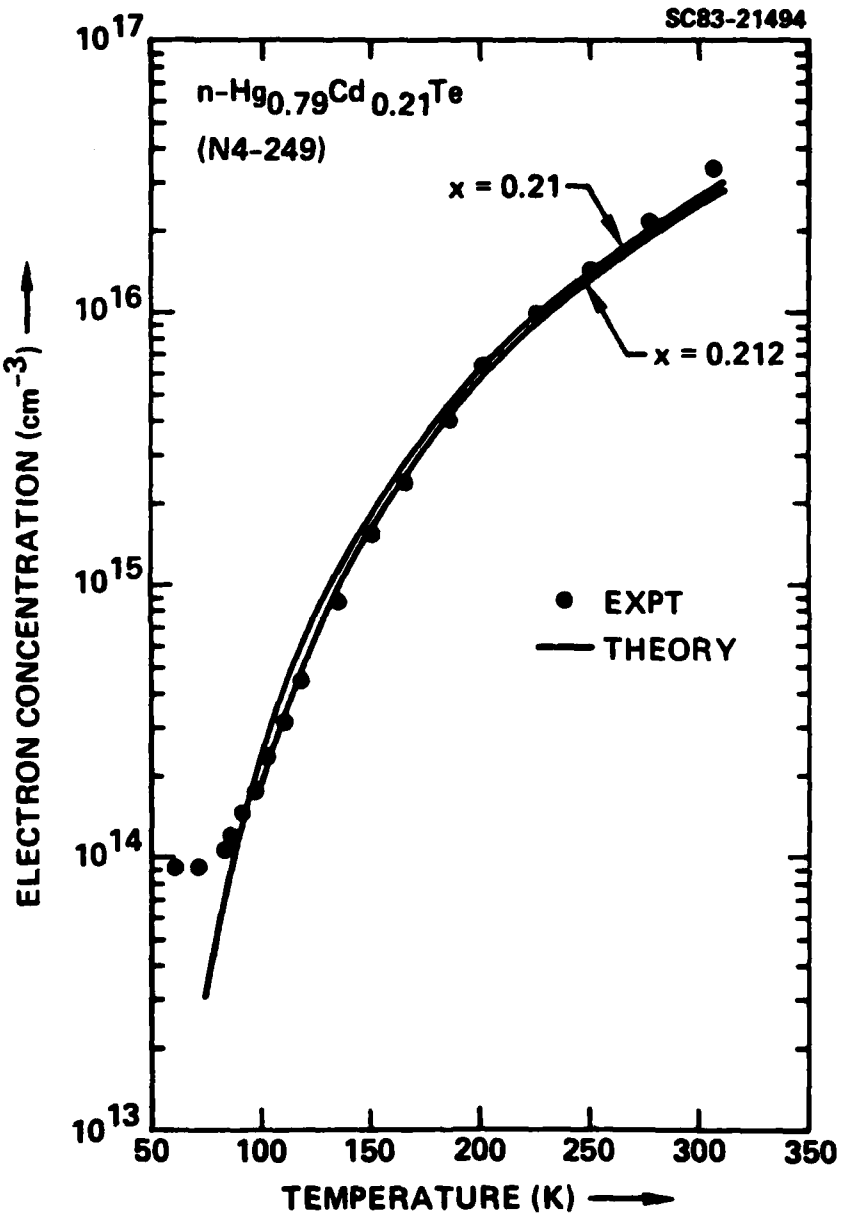

Fig. 8 Temperature dependence of electron concentration as obtained from Hall effect measurements for n-$Hg_{0.79}Cd_{0.21}Te$. The solid and dashed lines are theoretical intrinsic carrier concentrations obtained from the expression for $n_i(x,T)$ in Ref. 10 and Ref. 11, respectively.

For x ≈ 0.21 samples passivated with an anodic oxide, we have observed lifetimes in the 4-7 μs range. The measured lifetime as a function of temperature on one of the passivated samples is shown in Fig. 9. The solid lines are theoretical lifetimes calculated for x = 0.207 and using Nemirovsky's expression for $n_i(x,T)$. For T > 150K, the lifetimes are close to those observed in unpassivated samples, whereas at lower temperatures, the lifetimes are considerably longer because of reduced surface recombination.

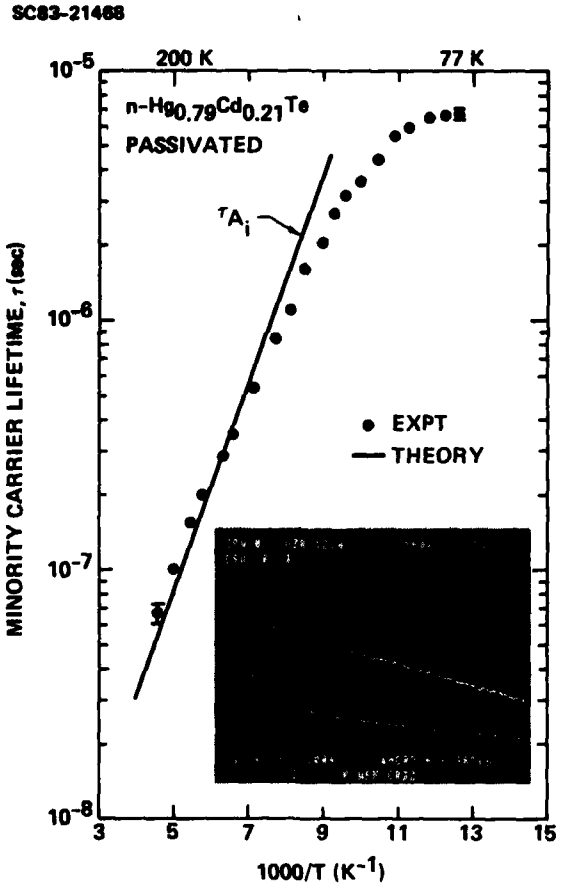

Fig. 9 Temperature dependence of minority carrier lifetime in passivated n-type $Hg_{0.79}Cd_{0.21}Te$. Theoretical values are obtained by using $n_i(x,T)$ in Ref. 10. The inset in the figure shows a typical photoconductive response. The lower trace is the decay curve and the upper one is the same trace plotted on a semilog scale.

From Figs. 7 and 9, it is clear that in the intrinsic region (T > 100K), the lifetime is limited by intrinsic Auger processes. In the extrinsic region, the lifetime is limited by Shockley-Read recombination and surface related effects.

2.3.2.2 p-Type LPE $Hg_{1-x}Cd_xTe$

Lifetimes in p-type HgCdTe at 77K are considerably shorter than in n-type. In p-$Hg_{1-x}Cd_xTe$ with unpassivated surfaces, the lifetimes measured are in general 15-20 ns at 77K and about 150 ns at 195K for x ≈ 0.21 material. A hole concentration (n_h) of 6×10^{15} cm^{-3} and hole mobility (μ_h) of 650 $cm^2/V\text{-}s$ at 77K are typical for these samples. The measured lifetime as a function of temperature for a typical x ≈ 0.21 p-type sample is shown in Fig. 10.

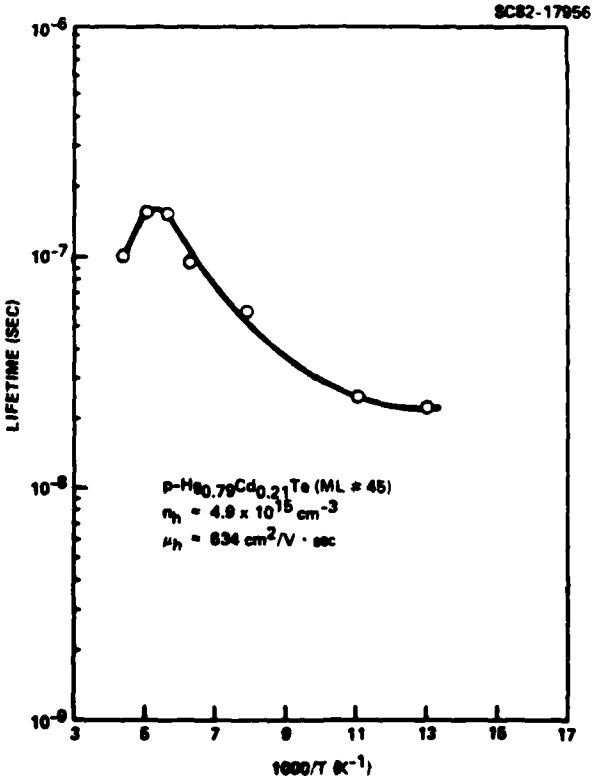

Fig. 10 Temperature dependence of minority carrier lifetime in unpassivated p-type $Hg_{0.79}Cd_{0.21}Te$. The solid line is for visual aid only.

The lifetime in LPE grown p-HgCdTe/CdTe is suspected to be limited by surface recombination. For example, the lifetime data we have observed on $x \sim 0.3$ material are very near that for $x \sim 0.2$ material. To further support this assertion, we carried out lifetime measurements with laser excitation through the CdTe substrate. In many samples, we observed a fast decay component ($\tau \sim 20$ ns) followed by a slow component with $\tau > 1$ μs. It is conjectured that the fast component is due to recombination at the interface and the slow component is due to true bulk recombination. The field due to the composition gradients near the interface is expected to enhance carrier diffusion into the bulk, which may explain why the bulk component has not been seen in photo-excitation of the p-type HgCdTe front surface. In addition, it indicates that surface passivation of p-HgCdTe by the CdTe substrate may be better than any conventional surface passivant used to date.

It is also possible that the slow decay component is due to presence of traps near the interface. This needs to be examined further by electrical and optical tests.

2.3.3 Summary

The minority carrier lifetime in n-$Hg_{1-x}Cd_xTe$ ($x \sim 0.2$) is comparable to that in bulk material. Above T > 100K, the lifetime is limited by intrinsic Auger recombination, and below 100K the lifetime is limited by Shockley-Read and surface-related effects. The lifetime in p-HgCdTe appears to be much more surface-dominated than in n-HgCdTe. We are beginning to see evidence for a longer lifetime by photo-excitation from the CdTe side, which is attributed to the bulk. However, the possibility of carrier trapping cannot be ruled out at this time. More definite conclusions may be reached when electrical measurements like DLTS and lifetime measurements by volume excitation using two photon absorption have been carried out. In our theoretical analysis of the lifetime data, we find that the expressions for energy bandgap and intrinsic carrier concentration given both by Nemirovsky et al and Hansen et al, yield a good fit to our data for $x \sim 0.2$.

3.0 CATION VACANCY FORMATION ENERGIES IN LPE $Hg_{1-x}Cd_xTe$

Experimental measurements of the cation vacancy formation energies (E_f) of $Hg_{1-x}Cd_xTe$ were carried out by Hg-annealing and rapid quenching to room temperature, followed by Hall measurements at 77K. Our observations show that one charge state vacancy is dominant, so that the fractional number, n, of cation vacancies at temperature T is related exponentially to the energy E_f required to create one vacancy, $n = A \exp [-E_f/kT]$. No appreciable temperature dependence of E_f due to temperature variation of the ionization levels and the self-consistent Fermi level is seen. Our measured value for the activation energy is found to be $E_f = 0.9 \pm 0.1$ eV, for $Hg_{1-x}Cd_xTe$ with x = 0.21, 0.3 and 0.43. This value is found to be nearly independent of Cd composition x. Theoretical calculations of the p-type carrier concentrations due to cation vacancies in $Hg_{0.8}Cd_{0.2}Te$ yield results which are in good agreement with experimental data. These modeling calculations predict the cation vacancies to be predominantly doubly ionized species at 77K.

Cation vacancies in $Hg_{1-x}Cd_xTe$ are thought to be responsible for the acceptor behavior in p-type conduction. Knowledge of cation vacancy formation energies (E_f) reveals important information about the p-type conduction, lattice defects, and temperature stability of electrical behavior. Measured values of E_f can also be compared with theoretical models of vacancy formation. Here we present the results of a study to measure E_f for a number of HgCdTe compositions by simple Hg-annealing/quenching and Hall measurements. The experimental analysis is based on several assumptions which are justified by theoretical calculations[13] as well as by arguments based on the experimental results.

From simple thermodynamic arguments, it can be shown that if one vacancy charge state is dominant, the fractional number n of cation vacancies in equilibrium at temperature T under the experimental conditions reported here is related approximately exponentially to an energy E_f referring to single vacancy formation:

$$n \simeq A \cdot \exp[-E_f/kT] \qquad (7)$$

where A is a constant for the material and k is the Boltzmann constant. The interpretation of E_f is given later (Eq. (14)). If we assume that either singly or doubly charged vacancies are dominant at 77K, after quenching, then the number of carriers contributing to the Hall concentration, which will be our measured quantity, is directly proportional to the number of vacancies n. The number of vacancies can therefore be studied quantitatively as a function of temperature from quenching experiments of HgCdTe samples.

The establishment of thermal equilibrium may require long times, especially at low temperatures where the mobility of the Hg vacancies becomes small. Quenching a crystal from a relatively high temperature T_q to a low temperature can freeze in the high temperature configuration of the atoms, thereby allowing the determination of vacancy concentration at $T \approx T_q$. Equation (7) may be used to determine E_f for cation vacancies from Arrhenius plots of carrier concentrations vs 1/T.

In the present study, experimental measurements of the E_f of $Hg_{1-x}Cd_xTe$ were carried out by Hg annealing and rapid quenching to room temperature, followed by Hall measurements at 77K. The variation of hole concentration was measured as a function of equilibrium temperature under Hg-saturated conditions. These results complement previously reported annealing data on bulk $Hg_{0.6}Cd_{0.4}Te$[14,15] and Hg loss rates and annealing experiments on $Hg_{1-x}Cd_xTe$.[16]

The $Hg_{1-x}Cd_xTe$ layers were grown by liquid phase epitaxy (LPE) on undoped CdTe substrates in the Te-rich solution. The thickness of the LPE layers was typically 20-25 μm. The as-grown samples without any chemical treatment were annealed in a saturated Hg atmosphere at 310-500°C for about 4 h. The sealed annealing tubes were then quenched in cold water. For Hall measurements, samples were cut in rectangular shape with typical dimensions 8×4 mm^2 and etched in 1% Br-methanol for 10 s. Electroless gold dots and indium solder were used for ohmic contacts to p-type $Hg_{1-x}Cd_xTe$. Samples were mounted in a liquid nitrogen dewar with GE varnish, and Hall measurements were carried out by the standard Van der Pauw method.

Experimental results for the E_f values for $x = 0.21$, 0.3, and 0.43 are summarized in Fig. 11. Note that the measured slope of the curves,

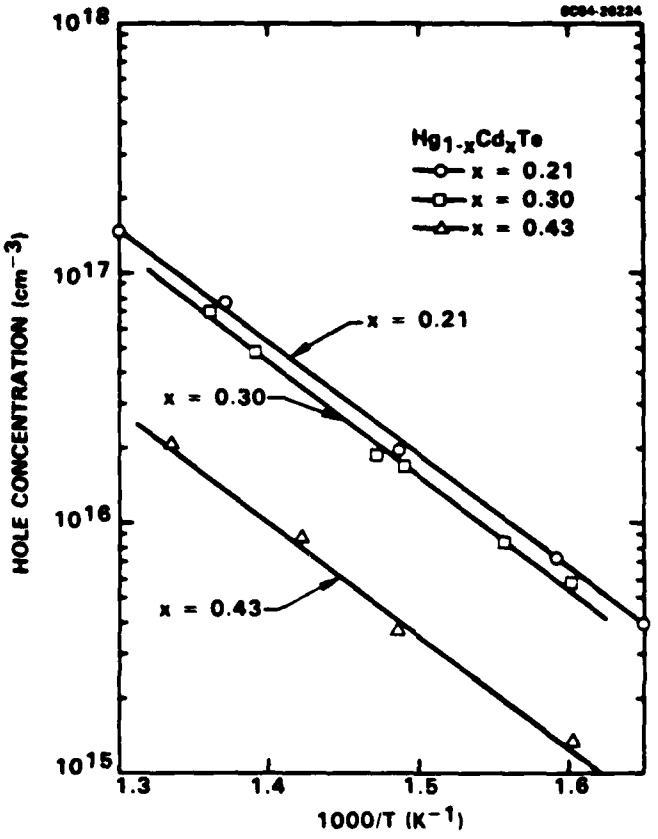

Fig. 11 Hole concentration as a function of Hg-annealing/quenching temperature for x = 0.21, 0.30 and 0.43 of $Hg_{1-x}Cd_xTe$.

E_f = 0.9 ± 0.1 eV, which we interpret as a cation vacancy formation energy in the $Hg_{1-x}Cd_xTe$ alloy under Hg-saturated conditions, is nearly independent of composition. The observed relative insensitivity of E_f to the composition parameter x may appear surprising, particularly in view of the differences in Hg-Te and Cd-Te bonding properties.[17] However, as discussed in Reference 13, many terms enter E_f, some of them significantly larger than the contribution of the broken bonds to the energy of the doubly ionized vacancy formation. It is important to note that E_f is not directly comparable to the values obtained by other workers[14,18] for enthalpies of cation vacancy formation under other

experimental conditions, since E_f refers to the enthalpy of cation vacancy formation under a saturated Hg overpressure, while in the other treatments the effects of varying the Hg pressure at a particular temperature are separated out.

Recently, Dimiduk et al[16] reported Hg loss measurements from $Hg_{1-x}Cd_xTe$ crystals by the He^+ ion backscattering method. From the temperature dependence of the number of Hg atoms lost per cm^2-s, activation energies ΔE were determined which ranged from 1.0-2.5 eV for x = 0.23-0.4. In this experiment, however, the measured values obtained by Hg loss rate involve motion of the Hg vacancies, as well as vaporization of Hg from the surface. Therefore, it is believed that the activation energy will include vacancy motion energy. Such ΔE would always be higher than the vacancy formation energies discussed in this work. It must be noted that our interpretation of the experimental data is based on a simple model of Hg vacancy formation.

In HgCdTe compounds, the generally accepted model (e.g., Kroger's model[19]) gives neutral, single and doubly ionized vacancies present in thermodynamic equilibrium. The formation of these vacancies at the Hg annealing temperature can be described by the reactions

$$Hg_{Hg} \xrightarrow{\Delta H} V_c^x + Hg\ (vapor) \tag{8}$$

$$V_c^x \xrightarrow{E_1} V_c^- + h^\bullet \tag{9.1}$$

$$V_c^- \xrightarrow{E_2} V_c^{--} + h^\bullet \tag{9.2}$$

$$[V_c^{TOT}] = [V_c^x] + [V_c^-] + [V_c^{--}] \tag{10}$$

where V_c^x is used for a neutral cation, vacancy V_c^- and V_c^{--} for singly and doubly ionized cation vacancies and $h^\bullet$ for a positively charged hole. For each reaction considered, we may write a mass action equation:

$$[V_c^x] = 3N \exp [-\Delta H/kT] \tag{11}$$

$$[V_c^-] = 2[V^x] \exp [-\{E_F(T) - E_1(T)\}/kT] \tag{12}$$

$$[V_c^{--}] = \frac{1}{3} [V^x] \exp [-\{2E_F(T) - E_1(T) - E_2(T)\}/kT] \tag{13}$$

where N is the total number of available cation lattice sites, ΔH is the Gibbs free energy to create a neutral cation vacancy in equilibrium minus kT ℓn3,[13] E_F is the Fermi energy, E_1 and E_2 are single and double ionization energies for cation vacancies.

We assume that the total concentration of cation vacancies is frozen in at 77K, and equal to the equilibrium concentration at the annealing temperature. We calculate the carrier concentrations at 77K by allowing the system to come to electronic equilibrium only; i.e., the distribution of vacancies among the various charge states is calculated self-consistently with the Fermi level. ΔH is given in Reference 1 as a function of x and T. It results from theoretical calculations using the dielectric model,[20] and not from an empirical fit. It is important to note that since the charged vacancies are dominant, the acceptor ionization levels and Fermi energy level at 77K are very important in determining the hole concentrations. We have used the the theoretical temperature dependence for the ionization levels assuming that they correspond to electronic orbits being quite localized rather than extended. We have found that a good fit to the data was obtained with zero temperature levels $E_1 = -0.505$ and $E_2 = 0.002$ eV, which correspond to the identification

of the E_2 level and the placement of the E_1 level below the valence band edge, a model suggested by C.E Jones.[21] This zero-temperature value for E_1 may seem excessively low. However, the first ionization level for cation vacancies in CdTe is 0.8 eV below the second at 300K,[21] so choosing E_1 to be 0.5 eV below E_2 in $Hg_{0.8}Cd_{0.2}Te$ may not be unreasonable if, as seems to be the case, the vacancy levels correspond to well localized states.

The calculated hole concentrations based on the above analysis of $Hg_{0.8}Cd_{0.2}Te$ at 77K are plotted in Fig. 12 and compared with those of experimental measurements on x = 0.21 $Hg_{1-x}Cd_xTe$ samples. Since mass action equations are only satisfied if the solid crystal has reached equilibrium with the saturated Hg pressures, the equilibrium concentrations of vacancies will be the actual concentration at the annealing temperature only if equilibrium is reached. In addition, when the crystal is quenched after high temperature annealing, the vacancies form complexes with other defects so that the total vacancy concentration at 77K may not be the equilibrium concentration at the annealing temperature. For these reasons it is useful to compare the 77K hole concentrations calculated from the dielectric theory to those measured in experiment. Hole concentrations calculated for x = 0.2 are in good agreement with the values obtained from Hg annealing followed by the 77K Hall measurements.

Since $Hg_{1-x}Cd_xTe$ is a highly ionic compound with ionicity of about 0.7, a cation vacancy is easily ionized. The calculations show that doubly ionized vacancies dominate both at the annealing temperature and at 77K. From Eqs. (7) and (13), we obtain an equation for the vacancy formation energy E_f, by means of an Hg escaping to the gas, in terms of thermodynamic parameters:

$$E_f = 2E_F(T) - E_1(T) - E_2(T) + \Delta H(T,x) \quad . \tag{14}$$

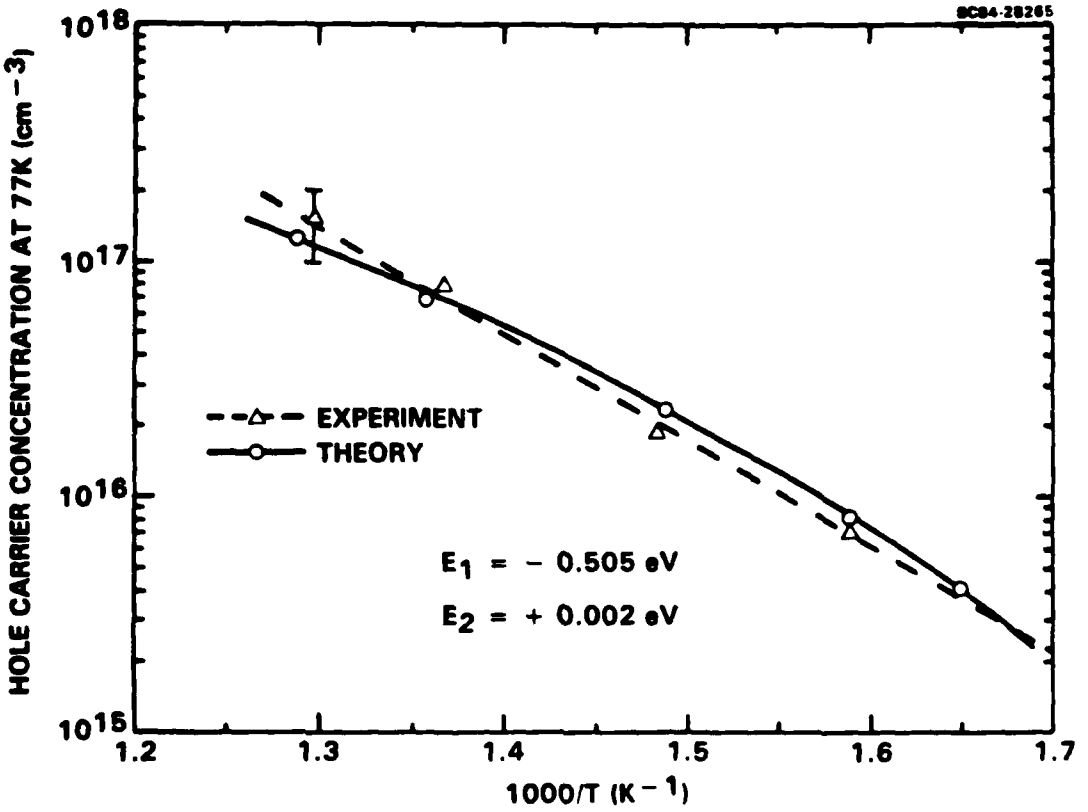

Fig. 12 Calculated hole concentration as a function of Hg equilibrium temperatures (solid curve) for x = 0.20 and the dashed line shows experimental points for x = 0.21.

It should be emphasized that this equation is valid only when V_c^{--} is the only important species as seen from Eq. (13).

Using the theoretical values for $E_1(T)$, $E_2(T)$ and $\Delta H(T,x)$, and the self-consistent Fermi energy $E_F(T)$,[13] gives a value for E_f very similar to that obtained from experiment, as shown by the agreement of the slopes in Fig. 12.

In conclusion, we have carried out experimental and theoretical investigations of cation vacancy formation in HgCdTe alloys of various compositions. The results can be summarized as follows:

A. Samples of $Hg_{1-x}Cd_xTe$ were grown by LPE, annealed (equilibrated) at high temperatures for long times under Hg-saturated conditions, and quenched rapidly down to room temperature. The p-type carrier concentrations in the samples were then taken as a measure of the concentration of cation vacancies.

B. Hall measurements at 77K of p-type carrier concentrations in HgCdTe quenched from various temperatures yield data which are consistent with simple modeling of vacancies. Arrhenius plots indicate activated processes and yield clear activation energies.

C. The activation energies, for what we interpret as the formation energy of cation vacancies by means of Hg escaping to the gas, is found to be $E_f = 0.9 \pm 0.1$ eV. Within experimental error, this value is also found to be independent of the composition parameter x of the alloys that were tried (x = 0.21, 0.3, and 0.43).

D. The experimental technique employed electrical measurements at low temperatures. The data, however, did not exhibit variations due to competing charge states for the vacancies, indicating that the vacancies are predominantly charged at 77K and are predominantly in a doubly ionized state at both the annealing temperature and 77K.

E. Theoretical calculations of the p-type carrier concentrations in $Hg_{0.8}Cd_{0.2}Te$ as a function of the quench temperatures yield results which are in good agreement with our 77K experimental data under the assumption of a large negative E_1 energy and a small positive E_2 state energy.

4.0 CHARACTERIZATION OF Te PRECIPITATES IN CdTe CRYSTALS

Te precipitates in CdTe have been characterized by transmission electron microscope (TEM), Auger spectroscopy, x-ray diffraction and Raman spectroscopy. The x-ray results show that the precipitated Te in Bridgman-grown Te crystals has the same structural phase as observed in elemental Te under high pressure. Auger and Raman microprobe spectroscopy were carried out to confirm Te precipitates in CdTe and identify the symmetry of the Te precipitates.

The formation of tellurium (Te) precipitates in CdTe is one of the most pressing materials problems in CdTe crystals. The need for high quality and defect-free CdTe with high optical transmission motivated a systematic study of this problem. Of particular interest is the nature of Te precipitates and their formation during the growth process of CdTe single crystals. The formation of Te precipitates is a consequence of the retrograde solid solubility in the CdTe binary system. Te precipitates are detrimental to a number of optical, opto-electrical and liquid phase epitaxy (LPE) HgCdTe substrate applications.

In order to grow high quality, defect-free HgCdTe layers, it is necessary to use high quality CdTe substrate material. Since the quality of LPE HgCdTe layers is strongly affected by the quality of CdTe, substrates with low dislocation density and high purity are required. Unfortunately, the CdTe substrates currently available have, in general, high dislocation density, varying from 10^3-10^8 cm^{-2}. During the past year, we have initiated a systematic investigation of structural defects in CdTe substrates by using transmission electron microscope (TEM). This study shows that dislocation nests, loops and stacking faults are prevalent in CdTe samples. The observed loops were verified to be the vacancy type and the stacking faults were generated from vacancy loops in the sample. Analysis of the electron diffraction pattern indicates that the sample purchased from II-VI Inc., is free of tellurium precipitation; however, Te precipitates have been observed in many other CdTe

samples grown by different techniques, e.g., traveling heater method, vapor transport technique and LPE CdTe grown from Sn solution. Relatively low dislocation density (< 10^3 cm^2) and apparent absence of stacking faults were observed in some vapor grown CdTe and LPE layers.

A significant improvement in quality of the sample has been observed on LPE CdTe grown on bulk CdTe in Sn solution. We do not see such extensive nesting and tangling of dislocations. In addition we do not see the prominent evidence we saw in some of the polished samples of scratch remnants remaining on the surface. However we do see some tellurium present as identified from selected area electron diffraction patterns and this seems to be prevalent in this THM (traveling heater method) CdTe wafer.

To study the nature of Te precipitates in CdTe crystals, we have carried out Auger analysis and x-ray diffraction studies. Undoped p-type CdTe wafers grown by the Bridgman method were cut into (111) orientaions, followed by mechanical polishing with 0.3 μm alumina powder and Br-methanol chemical etching. When viewed under an optical microscope, some CdTe substrates show inclusions of various sizes throughout the surface as shown in Fig. 13. These inclusions are also confirmed by IR transmission microscope examination. We recently carried out spatially resolved Auger analysis on these substrates. Figure 13 shows the Auger spectra from the relatively clear field of substrate labeled as A. Two distinct peaks, due to Cd and Te, are observed in the clear region. To understand the structure of the inclusions we first looked at the relatively small sized inclusions labeled as region B in Fig. 13. The magnitude of Te peak is nearly the same as obtained from CdTe sources, but the Cd peak is much weaker. The inclusions seem to contain small amounts of cadmium; however, they consist mainly of Te. Similarly, we probed the larger inclusions labeled as region C in Fig. 13. The Auger spectra shown in Fig. 13(c) again revealed Te precipitation. The Cd to Te peak intensity is nearly five times weaker.

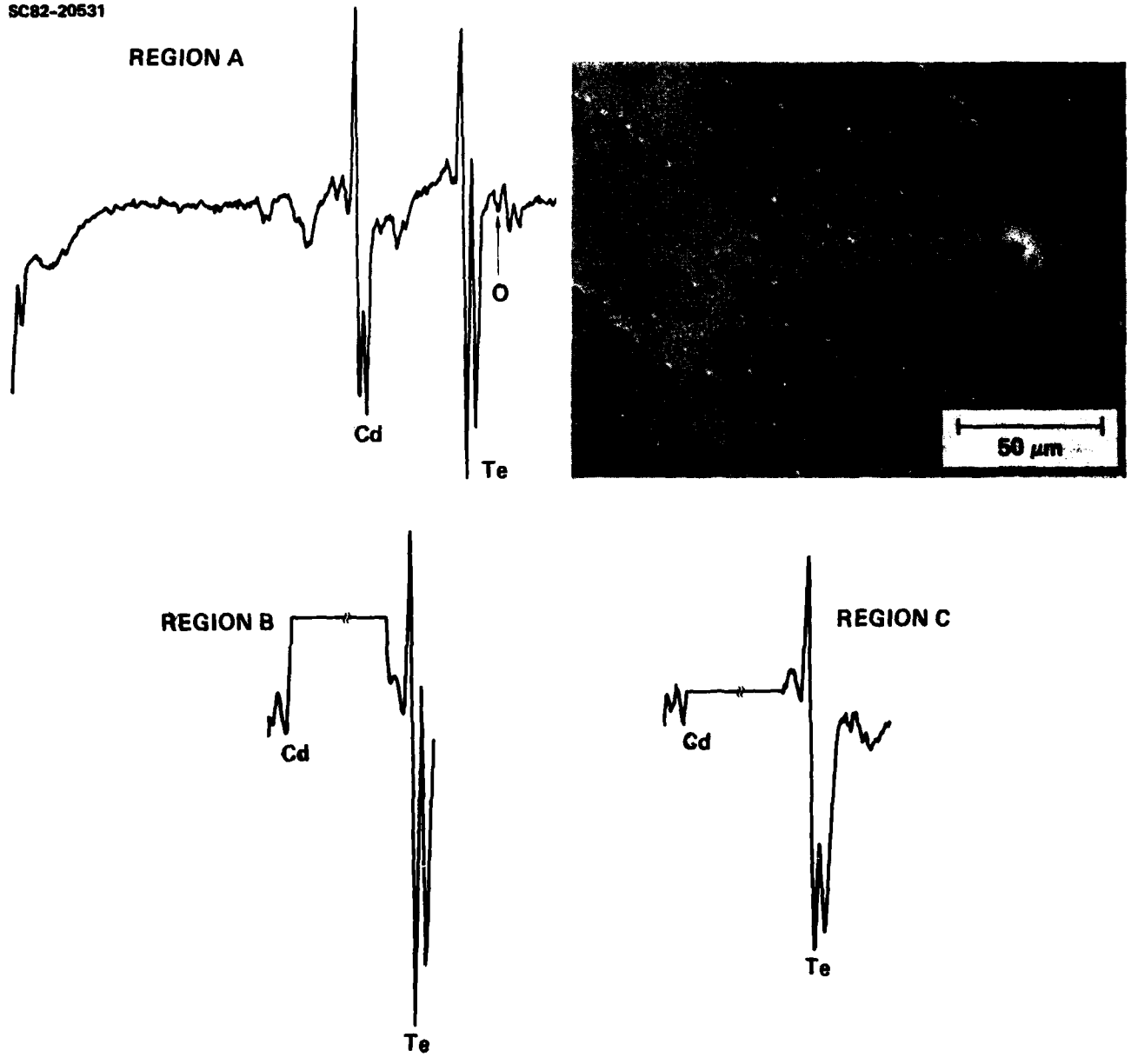

Fig. 13 Auger spectrum of a CdTe substrate exhibiting surface inclusions. The spectrum is for (a) inclusion-free CdTe, (b) small, and (c) large inclusions. Data shown in (b) and (c) were taken in the vicinity of Cd and Te peaks only.

In an effort to reduce the concentration of Te precipitates, a piece of CdTe was annealed in Cd overpressure at 600-800°C. Subsequent to annealing the optical microscope showed that the concentration of small inclusions was considerably reduced, whereas the larger ones were still present. The corresponding improvement of the infrared transmission due to Cd-annealing is shown in Fig. 14. The high transmission suggests that small Te inclusion may be responsible for low optical transmission.

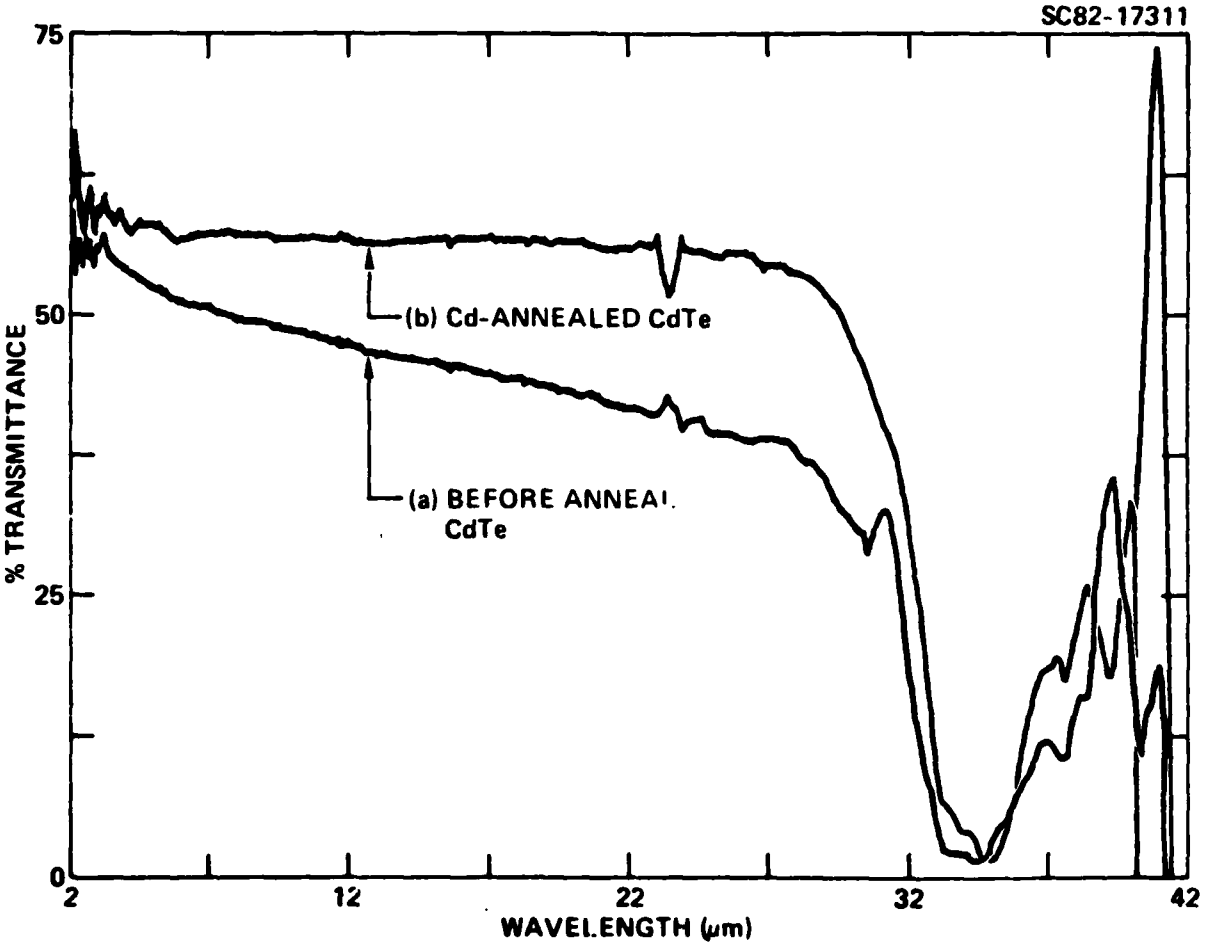

Fig. 14 Infrared transmission spectra of a CdTe substrate are shown before and after Cd annealing.

Another interesting feature of Cd annealed CdTe substrates is the impurity profiles. Figure 15 shows the SIMS depth profiles for four CdTe samples. All the CdTe samples are finished up by Cabosil polishing. The first sample (#1) is as-grown and Cabosil polished; its profile shows the CdTe surface to be heavily contaminated up to 10 μm deep. Only a few of the ions are indicated in this figure, but other impurities were also observed. The Cd annealed sample (#2) shows exceptionally low levels of Li (17), Na (23), Al (27) and K (39). This sample was etched about 20 μm prior to Cd annealing; the profile shows an exceptionally clean sample. Sample #3, which was Br-methanol etched after Cd annealing, again shows high levels of impurities, surface contamination is very noticeable. Sample #4 was annealed CdTe on which LPE HgCdTe was first grown and then polished off. The profile of sample #4 shows both surface contamination and high levels of background impurities. It is also noticed that all the Cd annealed samples (#2, 3 and 4) show very low levels of Li impurity compared to the unannealed sample.

The effects of Cd annealing are twofold. First, Cd annealing reduces Cd vacancies in CdTe and converts p- to n-type. A Li atom in CdTe acts as an acceptor when substituted on a Cd site, and as a donor when located interstitially. During Cd annealing, Li on a Cd site outdiffuses to the sample surface and is replaced by a Cd atom. Second, it has been observed that in II-IV semiconductors which exhibit anion precipitation phenomena, high temperature post-anneals have been successfully used to reverse these effects. A consequence of Cd annealing in CdTe is that reincorporation of Te precipitates occurs through the formation of CdTe. The transmission of CdTe wafers was significantly improved by reducing Te precipitate particles as well as cation vacancies. As a result of the Cd annealing, the quality of CdTe substrates is significantly improved.

To gain insight into the nature of Te precipitates in CdTe, we performed x-ray diffraction and micro-Raman scattering experiments. X-ray diffraction profiles for unannealed CdTe measured using Cu Kα radiation are shown

SC5305.6FR

SC82-19462

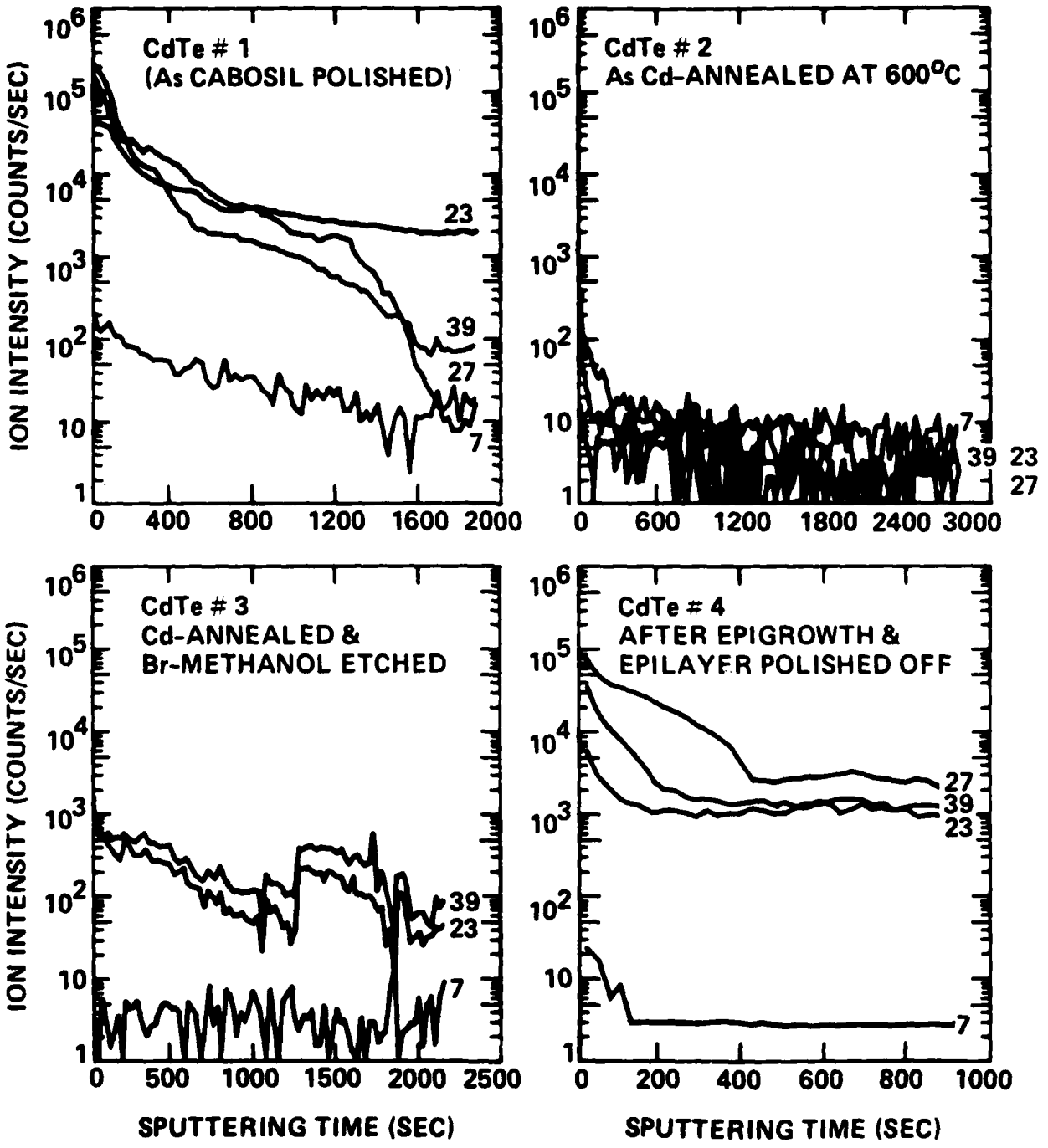

Fig. 15 SIMS depth profiles for four CdTe samples.

in Fig. 16. In both unannealed and Cd-annealed CdTe cases, the main diffraction lines for single crystal CdTe, namely (111), (222), (333) and (444), are present. Table 1 lists the diffraction lines and the d-spacings measured. Both the peak positions and d-spacings of main diffraction lines are in good agreement with x-ray powder file data for CdTe (111).

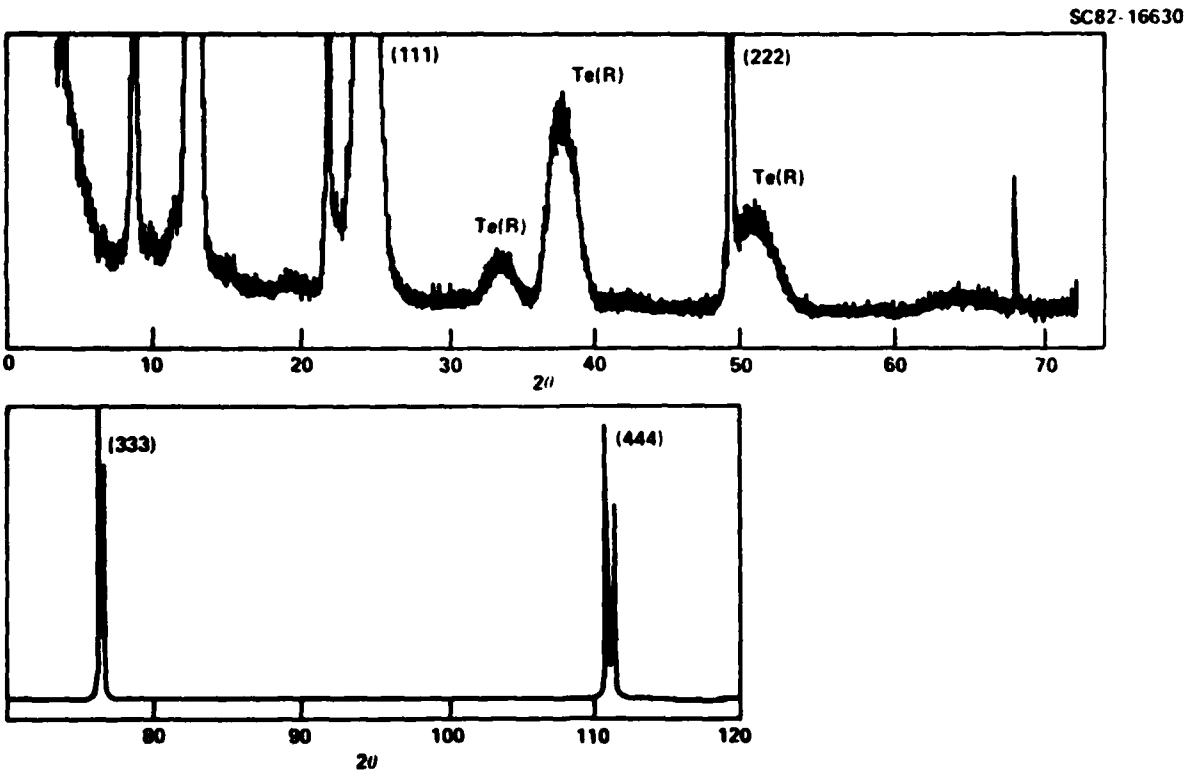

Fig. 16 X-ray diffraction spectrum for Bridgman-grown (111) CdTe before Cd annealing.

Table 2

Comparison of the Experimental d-Spacings of Tellurium Precipitates In CdTe and Powder Data for High Pressure Tellurium Phase

Peak Intensity (counts/s)	d_{obs} (A)	CdTe hkl	Te (115 kbar)* d(A)
125	7.25		
250	4.19		
625	4.15		
> 1,000,000	3.74	111	
100	2.73		2.78
425	2.44		2.36
2200	1.87	222	
100	1.84		1.78
89,000	1.248	333 α_1	
62,000		333 α_2	
75,000	0.9358	444 α_1	
49,00		444 α_2	

*Data of Jamieson and McWhan, Ref. 22.

The additional diffraction lines were initially suspected to be due to impurities like C, Fe, Cu, Cd, cadmium oxides and tellurium oxides. The lines could not, however, be associated with any of these impurities. We noticed also that these additional lines were not present in the Cd-annealed CdTe and other high transmission CdTe samples. The x-ray diffraction spectra shown in Fig. 16 show that the spurious diffraction lines are at 2θ value equal to 32.8°, 36.8° and 49.7°, corresponding to d spacings of 2.73, 2.44 and 1.84A. A comparison of these d-spacings with the data of Jamieson and

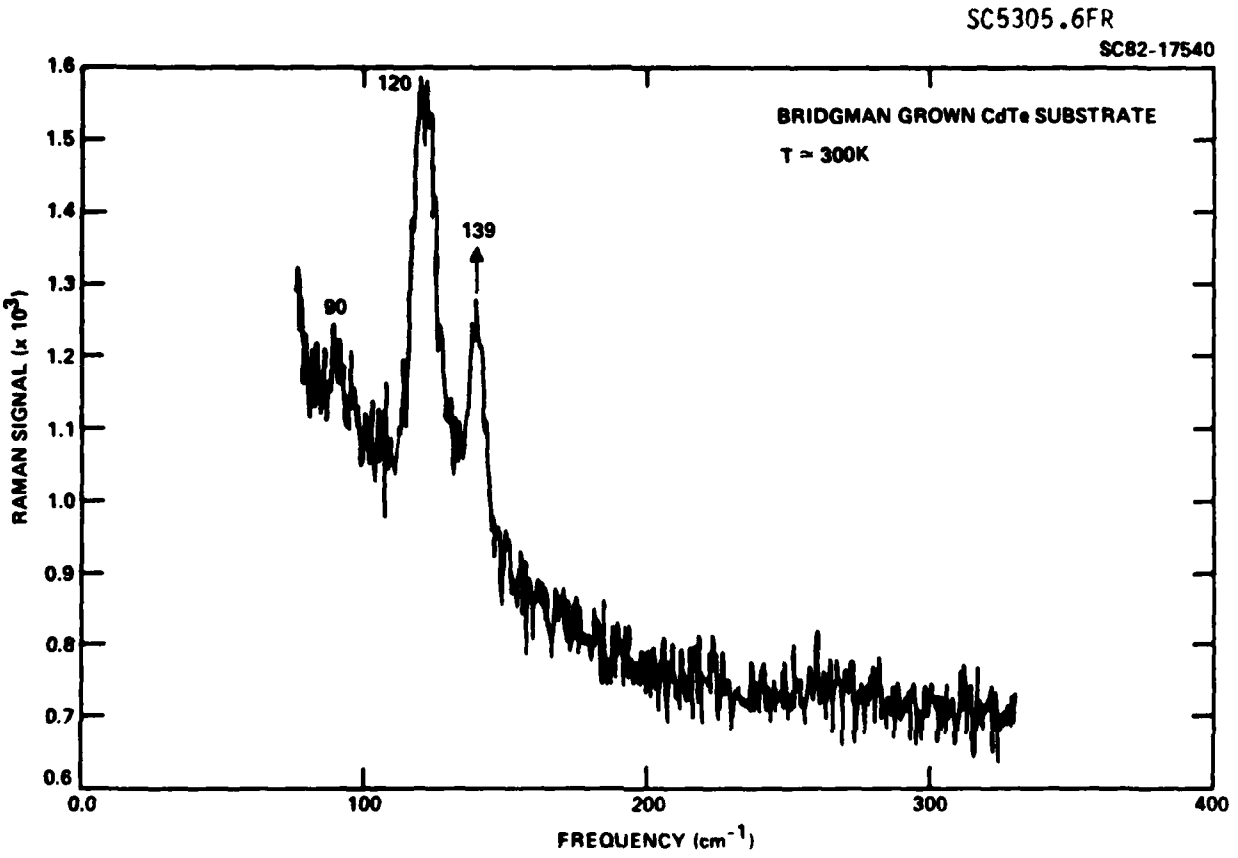

Fig. 17 Stokes micro-Raman spectrum of Te precipitates in CdTe crystal.

Chan's[22] suggests that the additional lines are due to Te precipitates, with Te in the high pressure rhombohedral phase. We have been unable to find another structure which unambiguously fits our data within estimated error of 0.5% in d/d_o.

Raman microprobe spectroscopy was also used to characterize Te precipitates in CdTe crystals.[23] The primary objective was to confirm Te precipitates in CdTe and identify the symmetry of the Te precipitates. Since Raman spectra of solids are obtained by the scattering of light by optical phonons, any scattering due to Te crystallites can be determined by comparing the results with those from a Te single crystal. Figure 17 shows a Raman spectrum from Te precipitates in CdTe at room temperature. A comparison of the intensity ratio and frequency positions of our observed spectra with the previously reported Te

spectrum[24] enabled us to identify the phonon lines. The three Raman active phonons correspond to one A_1 (120 cm^{-1}) and two E (90 and 139 cm^{-1}) modes. One interesting fact was that our observed Raman lines are approximately 2 cm^{-1} lower in energy than those reported for single crystal Te at room temperature. As discussed above, our x-ray results show that the Te precipitates in CdTe are in the high pressure phase, where similar shifts of the phonon lines may be expected.[25] This result is then consistent with the x-ray data.

In summary, we have identified the nature of Te precipitates in CdTe by Auger, x-ray diffraction and micro-Raman spectroscopy. The x-ray result shows that the precipitated Te in Bridgman-grown CdTe crystal has the same structural phase as observed in elemental Te under high pressure. Micro-Raman spectroscopy was carried out to confirm Te precipitates in CdTe and identify the symmetry of the Te precipitates.

5.0 EQUILIBRIUM OF NOBLE GASES Xe, AND He WITH $Hg_{0.79}Cd_{0.21}Te$

We have carried out experiments with annealing $Hg_{0.79}Cd_{0.21}Te$ in mixtures of a rare gas (Xe and He) and Hg atmospheres in order to examine p-type conduction mechanisms in HgCdTe alloys. The results were very interesting in that reduced hole (p) carrier concentrations and higher mobilities μ_p were observed, as predicted by an empirical model presented here.

5.1 Introduction

Impurity compensation in II-VI compounds has been the subject of intensive investigations.[26,27] The HgCdTe alloy system is particulary important since the bandgap can be tailored to match infrared detector requirements over a wide spectral range (1-25 μm). Cation vacancies in $Hg_{1-x}Cd_xTe$ are thought to be responsible for the deep levels associated with nonradiative recombination centers. Therefore, extensive research on the shallow p-type impurities doping (e.g., IB and V-group elements) is being conducted at many laboratories. Here we report on studies which explored the compensation effects of Hg-annealing of HgCdTe alloys in the presence of the noble gases Xe and He.

In a series of earlier studies discussed above in Section 3.0, we investigated the species responsible for p-type conduction in $Hg_{1-x}Cd_xTe$.[28,29] These studies strongly suggested Hg-vacancies as the dominant p-type species. The values obtained for vacancy formation energies E_f were nearly independent of the alloy composition parameter x. In order to study the Hg-vacancies in more detail, we decided to substitute some inert atoms in their sites. The noble gas Xe was selected for this purpose. Based on some initial arguments, we expected to see less p-type (or possibly low concentration n-type) conduction, and better mobility μ_p for HgCdTe annealed, and quenched in a Hg/Xe mixture, as compared with that annealed only in Hg atmosphere and quenched from the same temperature T_q.

The incorporation of noble gas atoms such as Xe into the intrinsic material defect sites has been studied in other semiconductors,[30] although positive proof will require further studies.

The interaction of Xe with HgCdTe is not only an interesting phenomenon, but studying it could help clarify the process of defect compensation in this important material system.

Here, we report on the effects of annealing in the presence of Xe/Hg mixtures on the electrical properties of $Hg_{0.79}Cd_{0.21}Te$. Our results can not be explained by means of a simple P-T phase diagram of HgCdTe at high temperature. We show that a satisfactory explanation of our data can be obtained by the assumption that Xe atoms substitute for the Hg vacancies in p-type HgCdTe and decrease hole concentrations, which are attributed to ionized cation vacancies. The Xe annealing experiments were subsequently followed by He-annealing experiments to further probe the rare gas-vacancy interactions.

5.2 Experimental

The $Hg_{0.79}Cd_{0.21}Te$ layers were grown by liquid phase epitaxy (LPE) from Te-rich solution on undoped (111) CdTe substrates. The thickness of the LPE layer was typically 30-40 μm. As-grown layers were p-type with hole concentration of 1.0×10^{17} cm^{-3} at 77K. For p-type $Hg_{0.79}Cd_{0.21}Te$ we have achieved low hole carrier concentration and high hole mobility by annealing at T_q = 410°C for 4 h under saturated Hg-overpressure and quenched rapidly to room temperature. Representative electrical properties of as-grown and Hg-annealed $Hg_{0.79}Cd_{0.21}Te$ epilayers are listed in Table 3. The hole concentration upon annealing was decreased an order of magnitude to about 1.7×10^{16} cm^{-3} and mobility improved to ~ 438 $cm^2/V\text{-}s$.

Table 3

Electrical Properties of $Hg_{0.79}Cd_{0.21}Te$/CdTe Epitaxial Layers
(T = 77K)

	As-grown	After Hg Annealing[b]	After Xe/Hg Annealing[b]
Conduction Type	p	p	n
Resistivity[d] (ohm-cm)	0.239	0.82	0.118
Hall Coefficient[a,c] (cm^3/Coul)	6.38×10^1	3.6×10^2	6.7×10^3
Hall Mobility (cm^2/V-s)	2.84×10^2	4.38×10^2	5.7×10^4
Carrier Concentration (cm^{-3})	9.1×10^{16}	1.7×10^{16}	9.3×10^{14}

[a] 6 KG magnetic field

[b] Hg-annealling was carried out at 405°C for 4 h in Hg atmosphere

[c] Top surface (~ 2 μm) was etched using 0.5% Br-methel solution before Hall Measurement

[d] Sample thickness was 40 μm.

In order to investigate the effect of Xe equilibrium with Hg vacancies, long wavelength infrared (LWIR) $Hg_{0.79}Cd_{0.21}Te$ was annealed at 410°C under a high pressure (~ 300 psi) mixture of Xe and Hg atmosphere. The electrical properties were measured after etching off the top surface (~ 2 μm) using 0.5% Br_2-CH_3OH solution. The results are also listed in Table 3. It was found that the test epilayer was converted into n-type whereas the control sample annealed under only a Hg environment remained p-type (the control and

test pieces were taken from adjacent pieces of the same epilayer). The electron carrier concentration and Hall mobility at 77K for the Xe/Hg annealed sample are unusually low, compared to well behaved n-type material (which is generally obtained by annealing at 200°C), suggesting the possibility of compensation.

The observed variation of the carrier concentration of Xe/Hg annealed epilayer as a function of temperature in the temperature range 20-300K is shown in Fig. 18. For comparison, we have also shown the behavior of a similar sample which has been annealed at 210°C, a temperature range at which standard n-type LPE HgCdTe is obtained. The temperature dependence of carrier concentration of a Xe/Hg annealed sample shows carrier freeze-out and mixed conduction which is a departure from classical n-type behavior. The electron concentration is nearly an order of magnitude lower than that for the only Hg-annealed sample at 210°C. A possible reason is that the concentration of Xe atoms equilibrated with HgCdTe is high enough to compensate the Hg vacancies and reduce the net N_A-N_D values. At increasing temperatures near the intrinsic region the electron carrier concentrations become comparable above 100K. In particular, Xe/Hg annealed sample shows thermal activation with ionization energy E_A = 1 meV in the temperature range 40-100K. The Hg-annealed sample does not show any freeze-out of extrinsic donor impurities like those of normal n-type HgCdTe alloys.

The difference in low temperature behavior of (410°C) Hg/Xe-annealed sample and (210°C) Hg-annealed samples is somewhat more pronounced in mobility measurements shown in Fig. 19. The Hall mobility of Hg-annealed sample increases with decreasing temperature from room temperature and at low temperatures becomes nearly independent of temperature at low temperatures. The electron mobility is mostly limited by ionized impurity scattering. In contrast, the mobility data of Xe/Hg annealed sample shows a peculiar behavior, possibly due to an additional defect scattering at near 100K.

SC5305.6FR

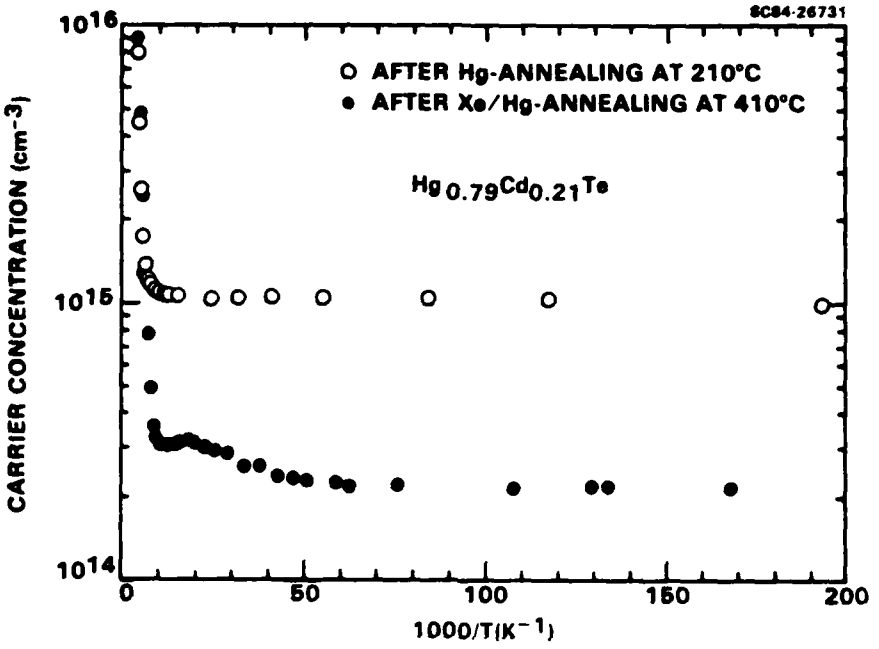

Fig. 18 Effect of Xe/He-annealing on carrier concentration of $Hg_{0.79}Cd_{0.21}Te$. Data for conventional low temperature Hg-annealed sample are also shown for comparison.

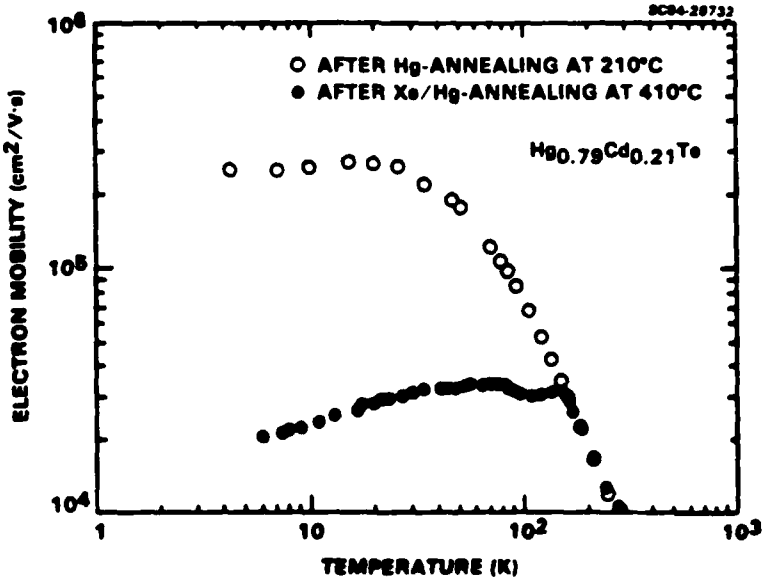

Fig. 19 Effect of Xe/Hg-annealing on electron mobility of $Hg_{0.79}Cd_{0.21}Te$. Data for a conventional low temperature Hg-annealed sample are also shown for comparison.

The anomalous behavior of carrier concentration and mobility in the Xe-annealed samples can be explained assuming that Xe atoms substitute for the Hg vacancies in p-type HgCdTe and a Xe acceptor level moves into the conduction band. Therefore, the Xe-annealed sample is compensated with Xe acceptors, and an acceptor activation energy greater than the band gap. As a result of a deep acceptor level with an activation energy comparable to the band gap, Xe-annealed HgCdTe converts to n-type with the complicated behavior of the Hall coefficients. If Xe atoms fill the Hg vacancies in p-type HgCdTe epilayers, the conversion of p- to n-type in HgCdTe systems[29] occurs due to residual donors (e.g., dislocations). These data, though not conclusive, and when combined with others,[30] can be used to propose a relatively simple model which may correctly describe n- or p-type conduction in HgCdTe. The predicted picture is consistent with much of the existing data on HgCdTe.

Let us assume that when HgCdTe is annealed at relatively low temperatures (~ 200°C at equilibrium with Hg overpressure), it becomes very low in cation vacancies. The conduction process at low temperatures is then dominated by native defects (e.g., dislocations or interstitials) or possibly some residual impurities. (If impurities, they must be common to all HgCdTe which is produced everywhere.) Assuming that these defects produce n-type behavior, low temperature annealed HgCdTe will be n-type with high mobilities ($\mu_n \sim 10^5$ $cm^2/V\text{-}s$) and carrier concentrations not exceeding $\sim 10^{15}$ cm^{-3}. Introduction of Hg-vacancies, i.e., by annealing at high temperatures, causes p-type conduction. For ordered and well annealed samples, the p-type carrier concentration obtained at high temperatures ($T_q > 300°C$) can be obtained by taking into account the vacancy formation energies $E_f \approx 0.9$ eV.[29] As described in Section 3.0, $Hg_{0.8}Cd_{0.2}Te$ is dominated by charged cation vacancies and ionization levels for cation vacancies cause large equilibrium concentrations of charged defects. One prediction of the above working hypothesis is that one can obtain lower than expected p-type (or possibly even n-type) carrier concentration, if the Hg vacancies are occupied by a neutral atom such as Xe. The addition of neutral atoms into the host crystal may affect the defect

equilibrium involved in the formation of extended defects. To test this idea, we also carried out an experiment annealing HgCdTe in He/Hg atmosphere.

Low level He doping was carried out by inert gas He and Hg annealing. About 1 atm (15 psi) He was filled into Hg-annealing samples and then $Hg_{0.79}Cd_{0.21}Te$ layers were annealed under a He/Hg atmosphere at 400°C for 4 h. The electrical properties were measured after etching off the top surface 2 μm thick HgCdTe layers. The results of hole carrier concentration and hole mobility of both Hg-annealed and He/Hg annealed $Hg_{0.79}Cd_{0.21}Te$ layers are plotted in Fig. 20 and Fig. 21. This study reults in consistently lower carrier concentrations and higher mobility than those in the Hg annealed samples under the same conditions for p-type LWIR HgCdTe. The hole carrier concentration and hole mobilities of the He/Hg annealed epilayers were in the range of (5-7) × 10^{15} cm^{-3} and (5-7) × 10^{2} $cm^{2}/V\text{-}s$, respectively. Noble gas interaction with Hg vacancies is believed to be responsible for the observed improvements. These results support the above consideration of Xe/Hg annealing effect that our samples with inert gas equilibrium had fewer Hg-vacancies, which may be due to substitution of Hg-vacancies by inert gas.

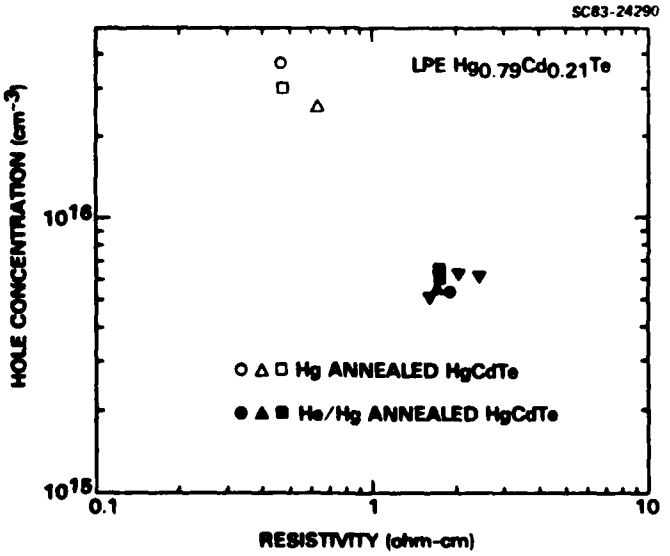

Fig. 20 Effect of He/Hg annealing on hole concentration of LPE $Hg_{0.79}Cd_{0.21}Te$.

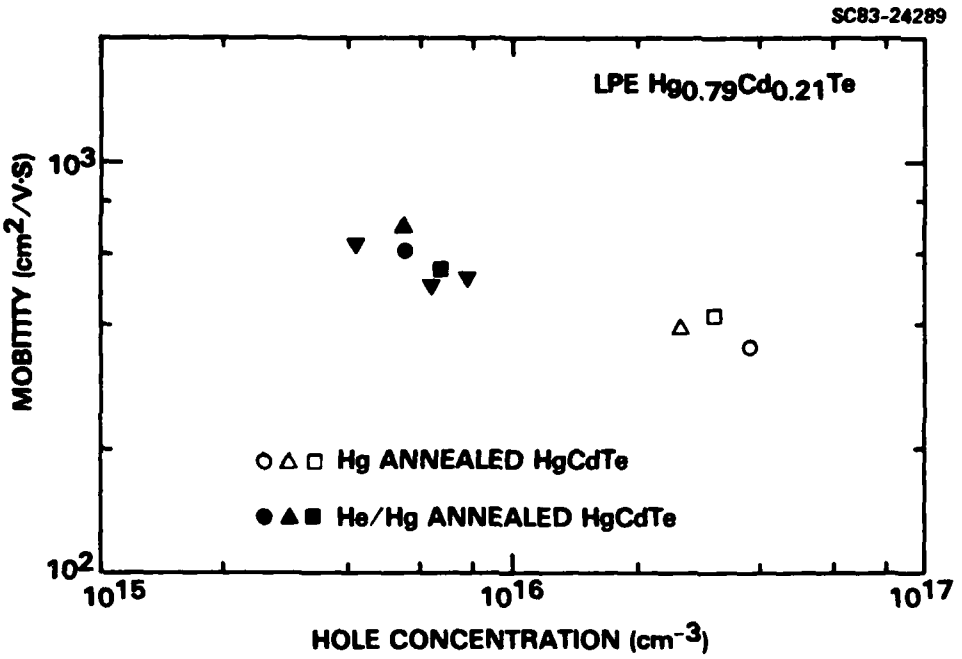

Fig. 21 Effect of He/Hg annealing on hole mobility LPE $Hg_{0.79}Cd_{0.21}Te$.

The results of He/Hg annealing experiments were very much in agreement with the predictions, i.e., consistently higher mobilities and lower p-concentrations were obtained. Substituting Xe in the vacancies drove the dominant conduction mechanism n-type. That is, the effective number of p-type centers went below that required to offset the residual n-type ($n \sim 10^{15}$ cm^{-3}). As expected, the control sample (Hg-annealed) remained p-type. The electron mobility in such Xe-compensated samples was lower than conventional (low temperature Hg-annealed) HgCdTe. However, we could not examine the hole mobilities.

Although the conclusions of our tests cannot be termed fully conclusive, the experiments do tend to support the hypothesis. With the admitted

inherent complexities of rare gases in solids, the results of Xe and He annealing experiments are surprisingly consistent with the simple working hypothesis. The assumption of rare gases diffusing in HgCdTe substituting for Hg vacancies is also consistent with recent experiments in Si.[30] Further experiments, particularly with varying ratios of rare gas/Hg, infrared spectroscopy or photoluminescence, are required for more definitive results.

6.0 PHOTOLUMINESCENCE IN CdTe AND LPE GROWN $Hg_{0.3}Cd_{0.7}Te$/CdTe

Photoluminescence (PL) is a standard technique to observe defects and impurities in semiconductors. The technique is very sensitive and the fact that it is nondestructive makes it very attractive for material screening. We have extensively studied PL of CdTe substrates because the quality of CdTe affects the growth of LPE HgCdTe. We have also studied PL of $Hg_{0.3}Cd_{0.7}Te$ and attempted to isolate defects in HgCdTe which propagate from the substrate during the LPE growth.

6.1 Bridgman Grown Bulk CdTe

The photoluminescence (PL) spectra of a wide variety of CdTe samples has been measured at 77K. It is found that the PL spectrum varies from sample to sample and may serve as a fingerprint of the quality of CdTe.

A typical spectrum of CdTe at 77K is shown in Fig. 22. It consists of two distinct lines. A narrow line peaked at 1.58 eV is intrinsic to CdTe and arises from recombination of excitons. The broad line is peaked at 1.42 eV and is believed to be due to donor-acceptor transitions[31] and is therefore an extrinsic property of CdTe. This line is also referred to as the defect line. The ratio of the peak intensities of the exciton (E) and defect (D) lines is a function of the sample. Simultaneous studies of other properties of these samples show that the samples which show a large ratio of E to D lines are of a better quality.

The transitions giving rise to the two lines are shown in the proposed energy level diagram in Fig. 23. When the electrons are excited to the conduction band, they relax to the lower energy states, either the exciton or the donor states. The ratio of the number of electrons falling into these two states appears to depend upon the concentration of donor levels. The excitons recombine to give the exciton luminescence and the electrons in the donor states fall into the acceptor state to give the broad defect line. In order to check that the defect luminescence is affected by the donor level

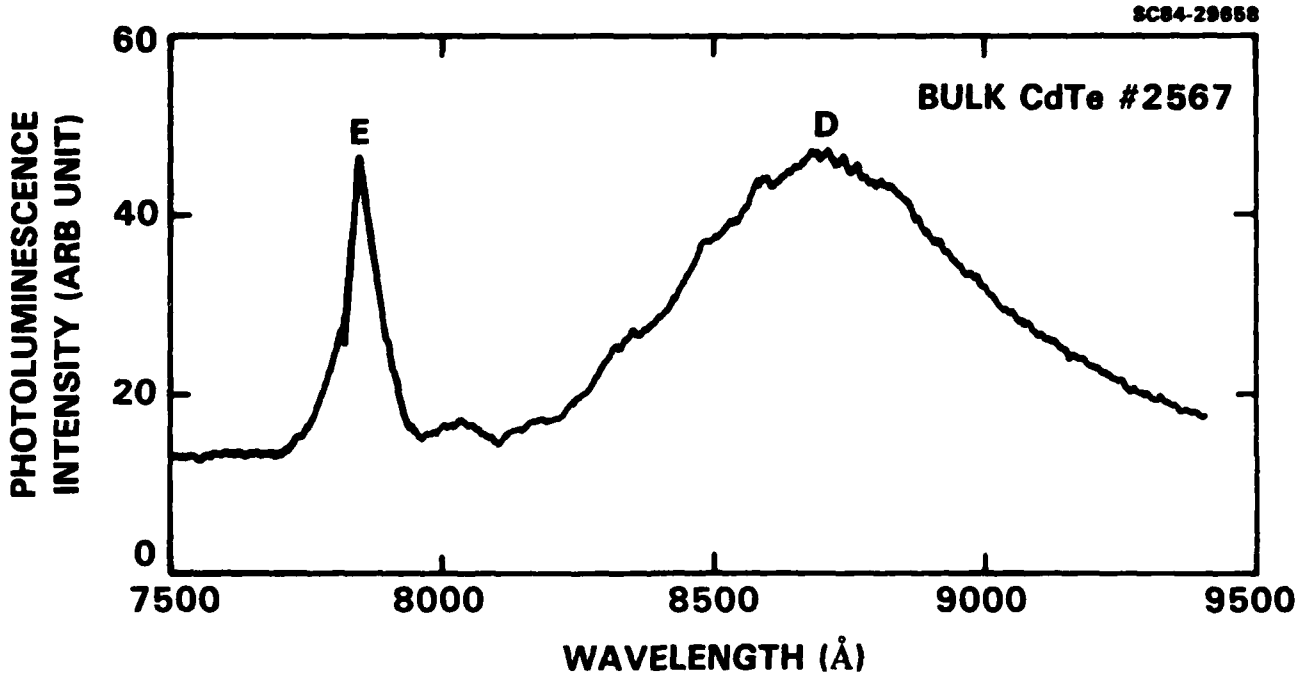

Fig. 22 Photoluminescence spectrum of undoped as-grown CdTe measured at 77K.

concentration, a sample of CdTe was deliberately doped with In to increase the number of shallow donors. It was found in the PL spectrum that the defect line luminescence increases by orders of magnitude relative to the exciton line. Also, annealing of CdTe in Cd atmosphere at 600°C for 3 days increases the defect line luminescence relative to the exciton luminescence. This is consistent with the enhanced defect luminescence in In-doped CdTe, since Cd annealing converts CdTe to n-type thereby increasing the number of donor states. Figure 24 shows the PL spectrum at 4.2K for both, unannealed and annealed CdTe samples.

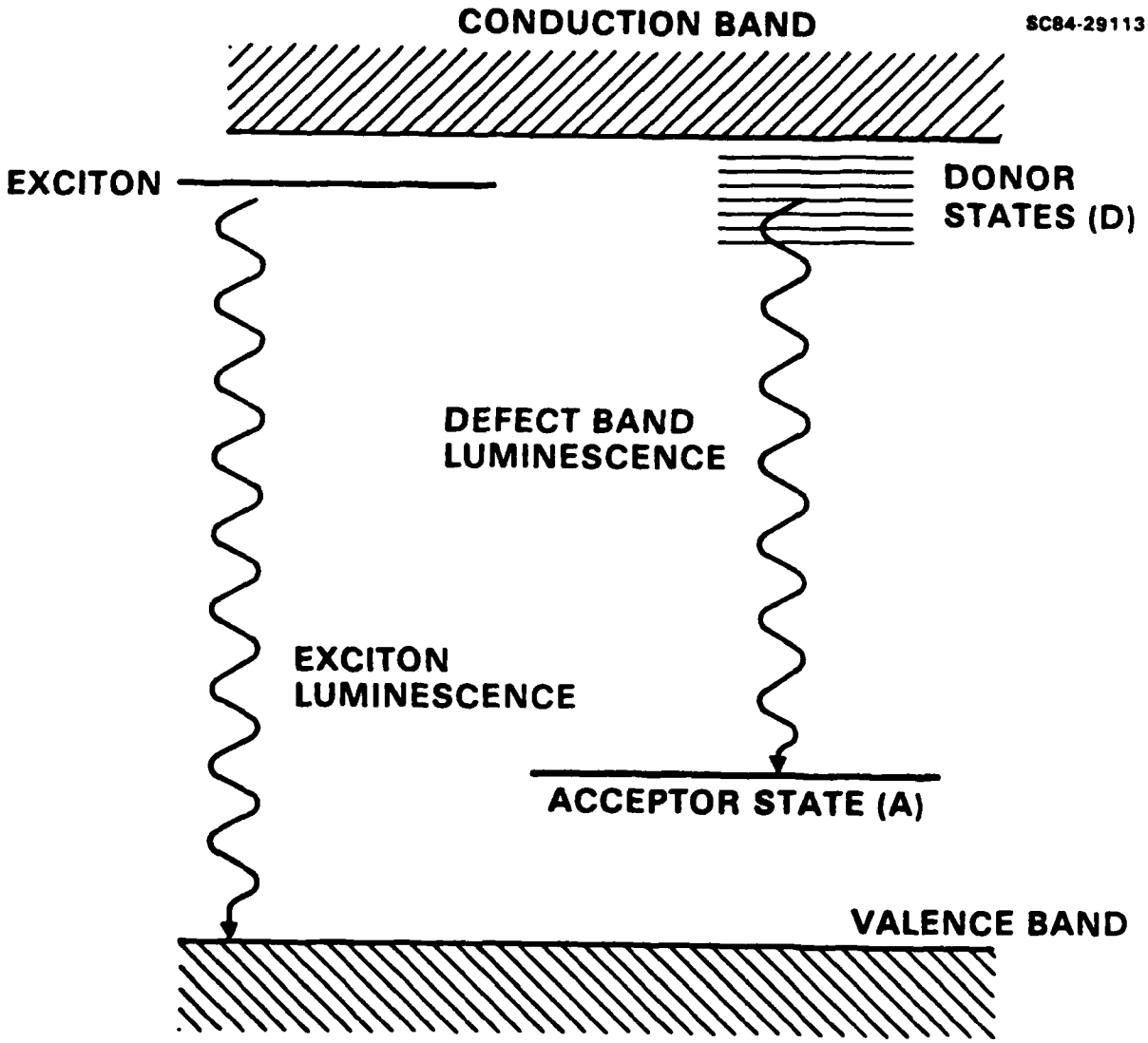

Fig. 23 Proposed energy level diagram of CdTe.

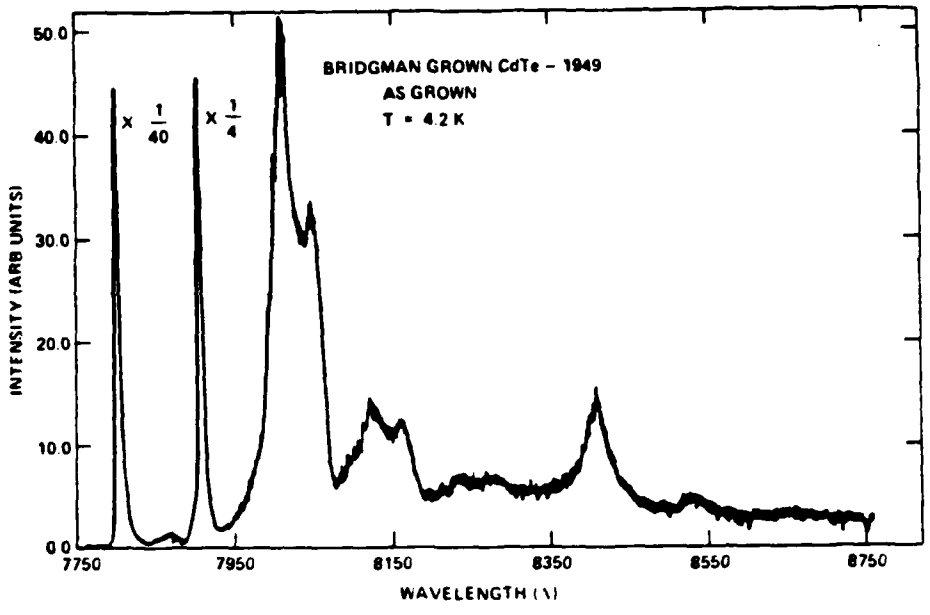

(a)

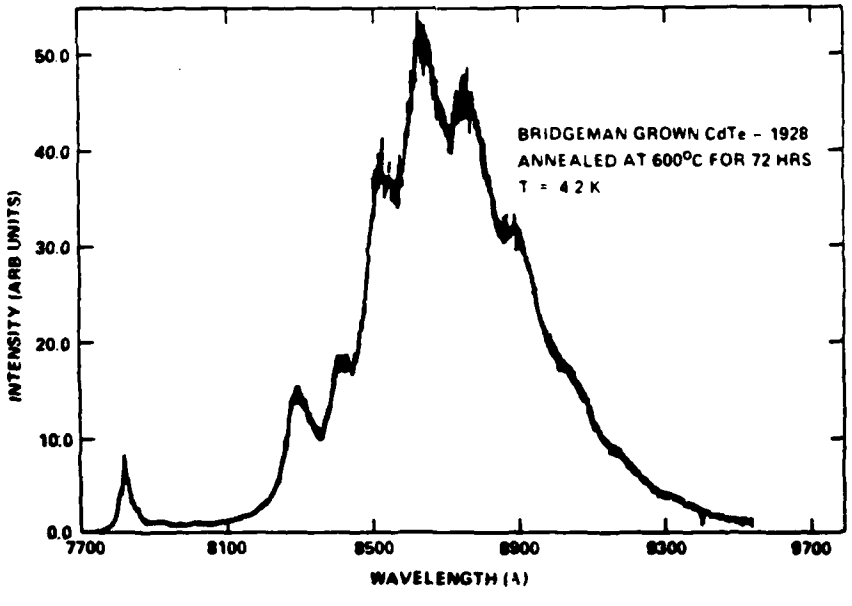

(b)

Fig. 24 Photoluminescence spectra of (a) as-grown and (b) Cd-annealed CdTe at 4.2K.

For unannealed sample there is no defect line present whereas the PL spectrum of annealed sample is dominated by defect level transitions. The details of the PL spectrum of unannealed sample is discussed in the next section.

6.2 LPE $Hg_{0.3}Cd_{0.7}Te$/CdTe

Photoluminescence was first applied to $Hg_{1-x}Cd_xTe$ by Elliot, Melngailis, Harman and Foyt who observed a pair of lines; they interpreted the energy difference between these two lines as the acceptor ionization energy.[32] Virtually identical results and interpretations were reported by Ivanov-Omskii et al.[33,34] Recently, Hunter and McGill observed a third line in bulk (x = 0.32 and x = 0.48) and liquid-phase epitaxially (LPE) grown (x = 0.5) material, which they suggested was bound exciton recombination;[35] most important they were able to identify the various lines by their shifts in position with temperature and by their dependence on excitation intensity. We observe different photoluminescence spectra from LPE-grown $Hg_{0.3}Cd_{0.7}Te$ and suggest a different interpretation of our spectra.

These HgCdTe epilayers were grown on CdTe substrates in a vertical dipping LPE system using a Te-rich solution. The films were all p-type, with typical hole density of 8×10^{15} cm^{-3} and hole mobility of 175 cm^2 V^{-1} s^{-1} at room temperature. All the samples are about 10 μm thick and were initially given a quick etch in a 1% Br/methanol solution. Then the samples were mounted in a cryogenic dewar and either immersed in liquid helium (2-4.2K) or liquid nitrogen (77K) or cooled in helium gas (5-75K). The samples were photoexcited by a cw Ar-ion laser beam (5145A), all of which was either reflected or absorbed by the HgCdTe epilayer. The luminescence was collected from the sample, focused in a 1/4-m grating monochromator and then detected by a cooled Ge photodiode. Some of the samples were removed from the dewar; their HgCdTe epilayers were etched away in a 5% Br_2/methanol solution; and then photoluminescence spectra of the remaining CdTe substrates were measured.

Figure 25 shows the photoluminescence spectra of $Hg_{0.29}Cd_{0.71}Te$ at4.2K photoexcited by 0.05 W of focused cw 5145A light. The spectrum at 4.2K

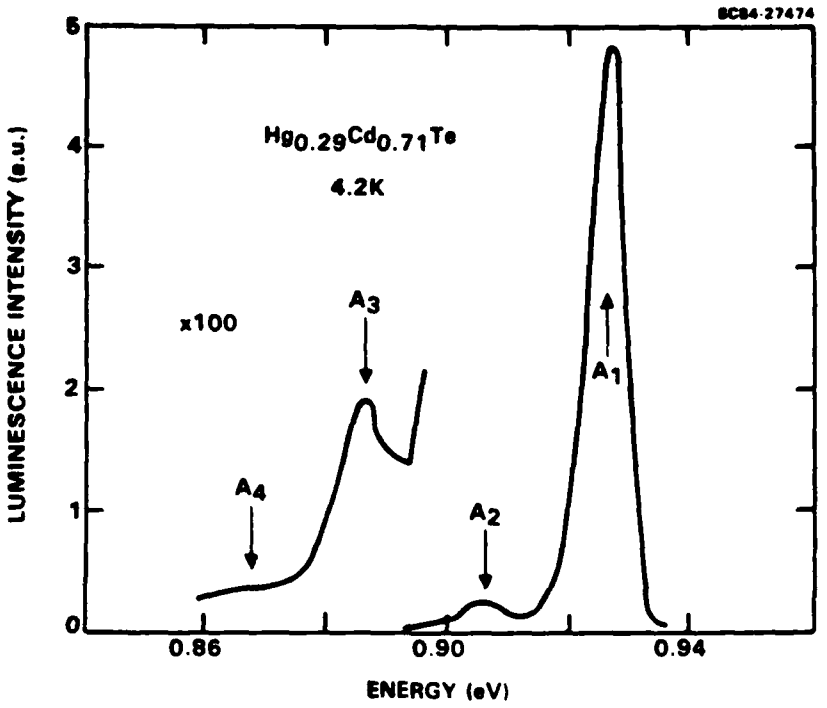

Fig. 25 Photoluminescence spectrum of $Hg_{0.29}Cd_{0.71}Te$ at 4.2K photoexcited by 0.05 W of focused cw 5145A light.

consists of a series of four peaks, A_1, A_2, A_3 and A_4, each separated by 20 meV - the LO phonon energy. The A_1 line is at 0.927 eV and its full width at half maximum (FWHM) is 5.7 meV. The A_1 line of $Hg_{0.31}Cd_{0.69}Te$ is at 0.896 eV and its FWHM is 6.3 meV. These spectra and lineshapes are unchanged when the sample temperature is reduced to 2K.

The different positions of the A_1 lines are due to different alloy compositions, since the band gap of $Hg_{1-x}Cd_xTe$ is a sensitive function of x. These differences in linewidth at low temperature are possibly related to the homogeneity of the epilayers, since changes in alloy concentration from one luminescent site to another will broaden the line.

Figure 26 shows the photoluminescence spectra of the CdTe substrates at 4.2K photoexcited by 0.05W of focused 5145A light. The spectrum at 4.2K consists of four features, two narrow lines B_1 and B_2 and two broad doublets C_1 and C_2. Both B_2 and C_2 are separated from B_1 and C_1 by 20 meV. All the lines in both HgCdTe and CdTe spectra that are shifted down in energy by multiples of 20 meV are due to electron-hole recombination with the emission of one or more LO phonons.

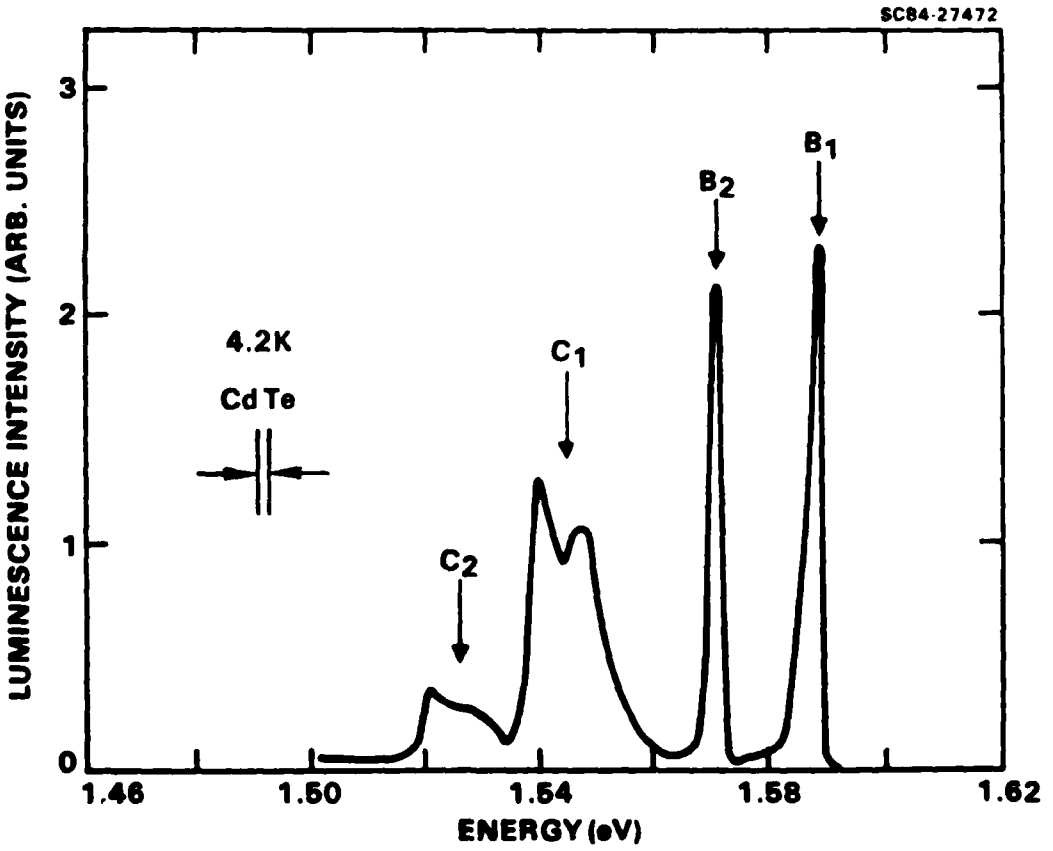

Fig. 26 Photoluminescence sprectrum of CdTe at 4.2K photoexcited by 0.05 W of focused cw 5145A light.

The C line at 1.538 eV in CdTe has been previously reported by Halsted and interpreted in terms of a donor-acceptor model.[36] The low temperature broadening of the C lines is then due to differing separation distances between donors and acceptors, giving rise to differing binding energies. More recently, the C lines in CdTe have been associated with displacements of Te atoms.[37-39] Narrow B lines at 1.593 and 1.575 eV in CdTe have been previously observed by Hiesinger et al. and interpreted as recombination from an exciton bound to a neutral donor.[40]

The tantalizing question is, what is the origin of the A lines in HgCdTe? Are they related to the B lines or C lines in CdTe? One might expect the same impurity to be present in both materials since both crystals are grown from the same elemental CdTe and Te metals. Or impurities from the CdTe substrate could diffuse into the HgCdTe epilayer during growth. From electron microscopy studies of the HgCdTe-CdTe interface by McGee and Woolhouse, dislocation lines were observed to propagate from the CdTe substrate into the HgCdTe layer.[41] One might expect radiative recombination at these dislocation lines in both materials.

In an initial effort to answer this question, we first measure the dependence of the A, B, and C lines on laser intensity in the hope of distinguishing between them. Unfortunately, over two orders of magnitude in laser intensity, the luminescence intensities of all three lines were approximately proportional to the laser intensity and the spectra unchanged and unshifted. In contrast, the lines observed by Hunter and McGill had nonlinear dependences on laser intensity and shifted to higher energy with increasing laser intensity.

Second, we measured the integration luminescence intensity of all three lines as a function of sample temperature, as shown in Fig. 27. All this data was taken with 0.05 W of unfocused 5145A light, in order to minimize heating effects. At higher temperatures, the integrated intensities of all three lines exhibited an exponential behavior with the following activation energies: ΔE_{A1} (x = 0.69) = 5.0 meV, ΔE_{A1} (x = 0.71) = 5.2 meV, ΔE_{B1} = 6.5 meV and ΔE_{C1} = 2.1 meV. In order to come to any conclusions, the binding energy of the

electron-hole pair has to be calculated. This is an extremely difficult calculation, but it can be roughly approximated by the free exciton energy

$$\Delta\Sigma = -\frac{\mu^* e^4}{2\epsilon_0^2 \hbar^2} \quad , \tag{15}$$

where $1/\mu^* = (1/m_e^*) + (1/m_h^*)$ is the effective reduced mass, ϵ_0 is the static dielectric constant. The relevant quantity is the ratio of $\Delta\Sigma$ for $Hg_{0.3}Cd_{0.7}Te$ to $\Delta\Sigma$ for CdTe

$$\frac{\Delta\Sigma_{HgCdTe}}{\Delta\Sigma_{CdTe}} = \frac{\mu^*_{HgCdTe}}{\mu^*_{CdTe}} \frac{\epsilon^2_{CdTe}}{\epsilon^2_{HgCdTe}} = 0.53 \quad , \tag{16}$$

which has been calculated from the known values of μ^* (Ref. 42) and ϵ_0.[43] For comparison,

$$\frac{\Delta E_{A1}}{\Delta E_{B1}} = 0.78 \quad , \quad \frac{\Delta E_{A1}}{\Delta E_{C1}} = 2.4 \quad . \tag{17}$$

Third, we measure the shift in the peak positions of these lines as a function of temperature, as shown in Fig. 28. The shifts to lower energy of the A_1 and B_1 lines are in agreement with the decrease in the bandgap with increasing temperature.[44] The opposite movement of the C_1 line is difficult to explain.

Clearly, from the temperature dependence of both the integrated intensity and the peak position, the A lines are not related to the C lines. The impurity or defect responsible for the C lines is not present in the epilayer, to within the experimental sensitivity of our photoluminescence system. It is very possible that the A lines and B lines are related; they could both be bound exciton recombination from the same neutral donor.

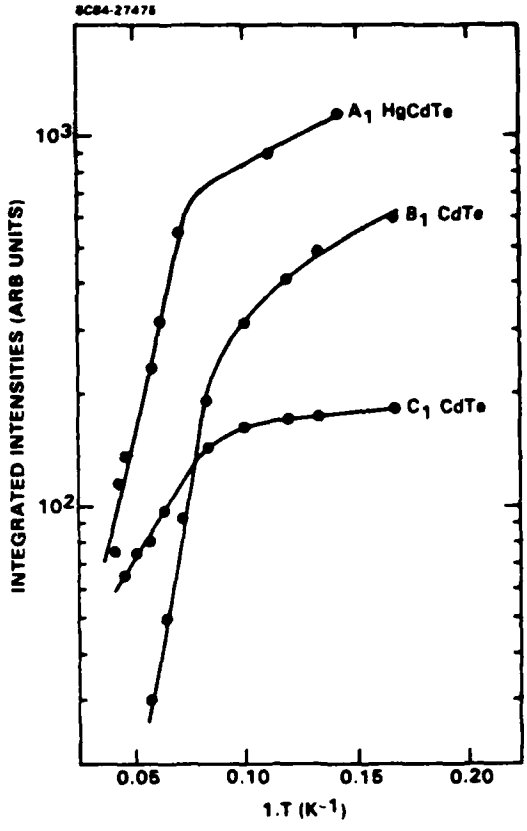

Fig. 27 Integrated intensities of the A_1 line $Hg_{0.31}Cd_{0.69}Te$ and the B_1 and C_1 lines in CdTe as a function of inverse temperature 1/T.

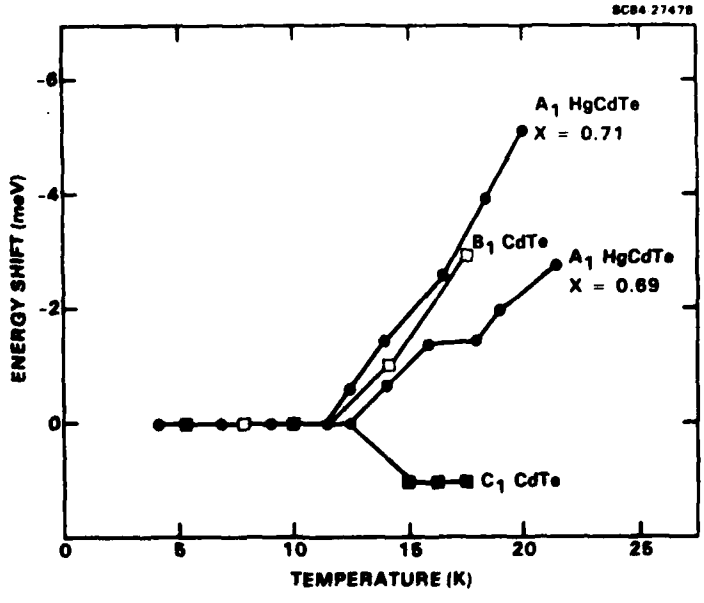

Fig. 28 Shifts in peak positions of the A_1 line in $Hg_{1-x}Cd_xTe$ (●) and the B_1 (□), and C_1 (■) in CdTe as a function of temperature. The shifts are measured with respect to their positions at 4.2K.

The most convincing way to establish this relationship between A and B lines would be to measure the photoluminescence spectra of various alloys between CdTe and $Hg_{0.3}Cd_{0.7}Te$ and plot the activation energy as a function of x. These samples are not presently available to us, but we plan to grow them in the near future. Another approach could be in the theoretical area. Osbourn and Smith have calculated the binding energy of an exciton bound to a neutral acceptor.[45] Their binding energies are much larger (30-60 meV) than those experimentally observed by us and strongly dependent on the potential chosen, but they decrease with decreasing x. It would be valuable to extend this calculation to excitons bound to neutral donors.

7.0 FAR INFRARED ABSORPTION SPECTRA OF CdTe and CdTe:Cu

Infrared absorption measurements at helium temperatures have been carried out on undoped CdTe and CdTe doped with different impurities. The purpose of these experiments is twofold: first to determine which site on the CdTe lattice do various impurities occupy and second to identify the energy levels associated with various impurities and use these identifications to isolate the residual impurities in nominally undoped samples.

All measurements are made on a Nicolet FTIR spectrometer with a resolution of less than 0.1 meV. The samples are typically 800 μm thick and are cooled to He temperatures using a Helitran.

The absorption spectrum of CdTe:Cu is shown in Fig. 29(a). The region between 125 meV and 200 meV shows sharp features and is shown on an expanded scale in Fig. 29(b). Three features of the absorption spectra are:

1. A broad band below the bandgap.

2. Several sets of sharp transitions, each set separated by 21.2 meV which corresponds to LO phonon energy at the zone center. The different sets are merely phonon replicas.

3. Each set consists of three sharp lines each separated by a constant energy of nearly 3.6 meV.

SC5305.6FR

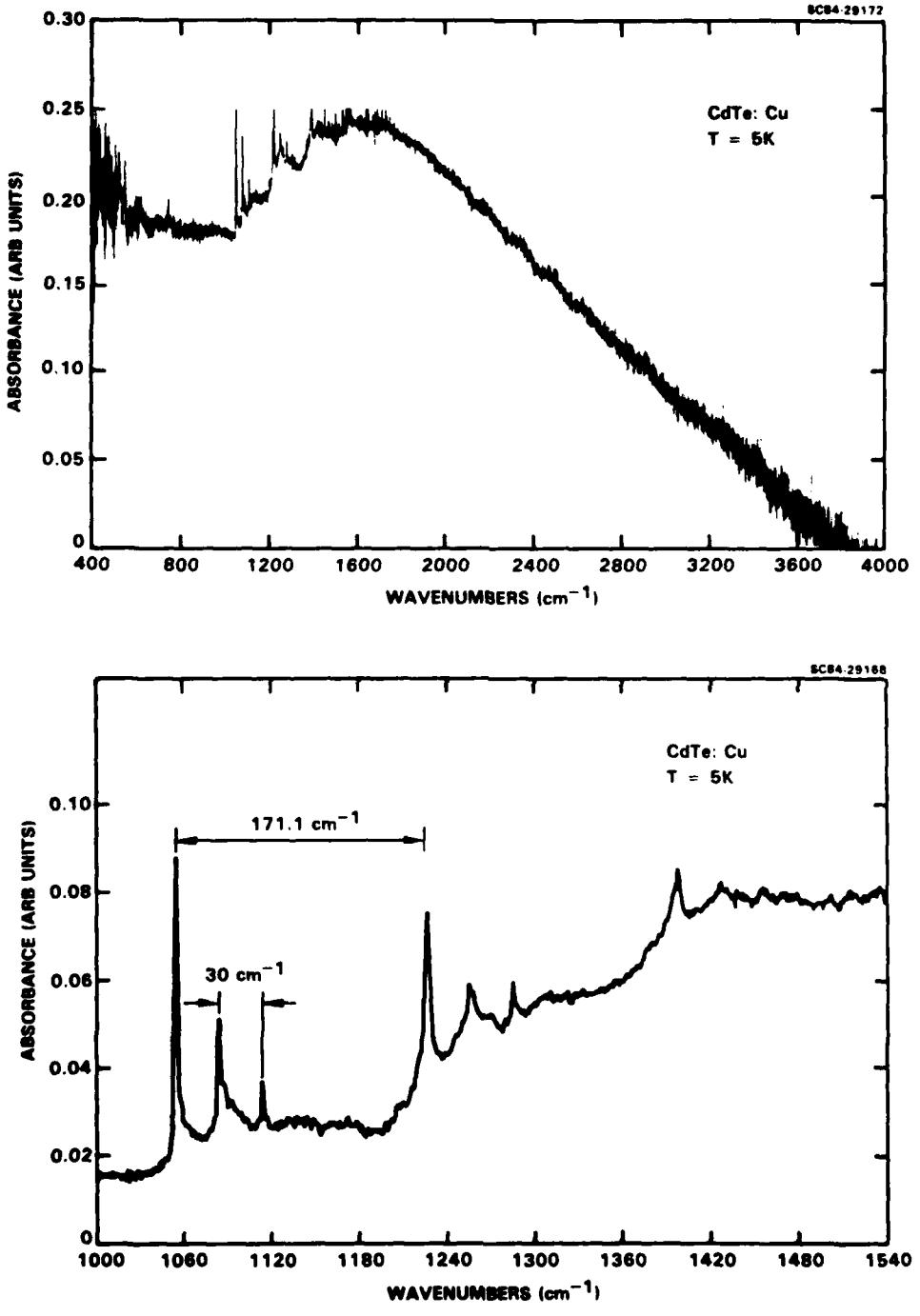

Fig. 29 Absorption spectra of CdTe:Cu at 5K. (a) A full spectrum, (b) the region between 1000 to 1540 cm^{-1}.

Infrared absorption spectrum of Cu doped CdTe has been studied earlier by Molva et al[46] and Furgolle et al.[47] Molva et al report peaks between 1000 and 1500 cm^{-1}, though not as sharp as in our spectrum, and interpret these lines as transitions between excited states of Cu acceptors. Furgolle et al have observed sharp lines as we do but on nominally undoped CdTe. They, however, associate the strong line in the triplet to a complex involving one group III donor and one cadmium vacancy. The other two lines in the triplet are interpreted as phonon replicas involving softened TA phonons.

In view of the strong transitions we observe in Cu doped CdTe which are not present in undoped CdTe or CdTe doped with other impurities, it is conceivable that the samples used by Furgolle et al had a large residual background of Cu acceptors. Assuming, therefore, that the sharp structure is related to the presence of Cu in CdTe we suggest the following origin of these transitions. The Cu acceptor occupied the Cd position as Cu^{++} with a $3d^9$ core. The $3d^9$ atomic manifold splits due to the host crystal field. The degeneracy of these split levers is further due to the Jahn-Teller effect. We believe the strong line in the triplet is related to a transition between d levels of Cu^{++}. The sharpness of the lines supports this argument as opposed to transition between excited states of Cu impurities being responsible for the absorption line. The other two lines in the triplet appear to be replicas of the strong line associated with the emission of 30 cm^{-1} energy quanta. The lowest characteristic phonon energy in CdTe is 35 cm^{-1} for the TA phonon at zone boundary.[48] It appears that the energy quanta of 30 cm^{-1} in Cu doped CdTe is modified TA phonon energy lowered due to weakened force constants around the impurity.

The electronic shell structure for Au and Ag is similar to that of Cu. We are therefore preparing samples of CdTe doped with these impurities for infrared absorption measurements. This should help answer whether we observe d level transitions or transitions involving excited states of impurities.

We have also measured absorption spectra in the low frequency region of up to 180 cm^{-1}. For Sample No. 1949, a high purity undoped CdTe sample, the

absorption spectrum is shown in Fig. 30. The lines peaked near 200 cm^{-1}, 250 cm^{-1}, 295 cm^{-1} and 307 cm^{-1} are observed in both undoped and doped samples and appear therefore to be intrinsic to CdTe.[49-51] The two strong lines near 360 cm^{-1} and 380 cm^{-1} are observed only in the high purity undoped CdTe No. 1949. The lines are also observed in Cu doped CdTe but are extremely weak.

The intrinsic lines are most likely multiphonon lines, a final assignment should, however, wait until we extend our measurements to even longer wavelengths and be able to see single phonon excitations. The extrinsic property of CdTe (e.g., defects) responsible for the lines at 360 cm^{-1} and 380 cm^{-1} is not known yet.

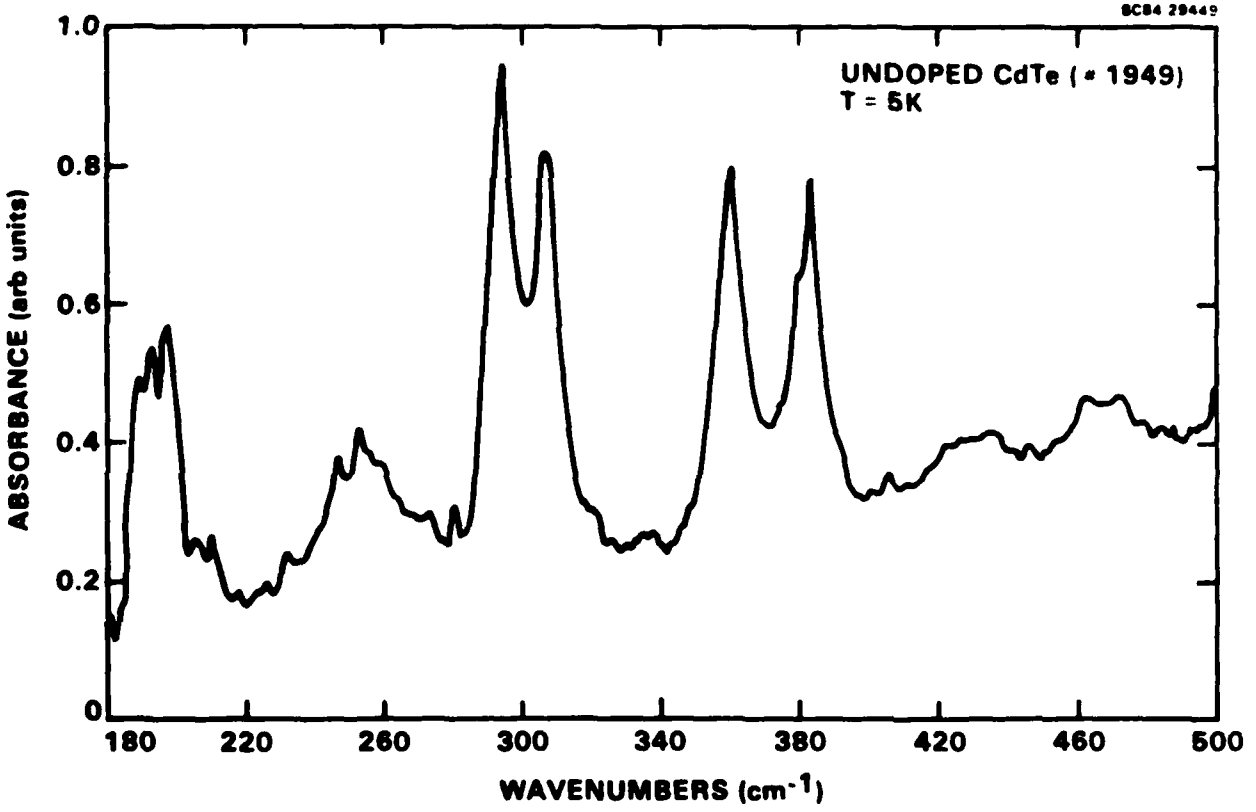

Fig. 30 Absorption spectrum of undoped as-grown CdTe in the region 180 to 520 cm^{-1} showing multiphonon structures.

8.0 ADMITTANCE STUDIES OF LPE $Hg_{0.7}Cd_{0.3}Te$

Admittance measurements have been made on p-type LPE $Hg_{1-x}Cd_xTe$ epilayers with $x \simeq 0.3$. Admittance spectra for these samples show the presence of two majority carrier (hole) traps. The hole trap levels in one sample (3-524) were 13 and 40 meV, and 23 and 70 meV for the other sample (4-31). Hall measurements were used to verify the lowest energy level of the acceptor. Dependence of the acceptor ionization energy on hole concentration suggests that the shallow level is associated with native defects controlled by Hg vacancies rather than impurities. In this section we describe the details of these measurements in the context of other published data.

Recently, Scott et al.,[52] reported electrical and far-infrared optical properties of p-type $Hg_{1-x}Cd_xTe$ with x in the range of 0.2 - 0.6; the acceptor ionization energy was 14 ±1 meV. More recently, Polla, Scott and Jones[53] reported deep imurity levels in p-type $Hg_{1-x}Cd_xTe$ by various deep-level spectroscopy techniques. Their results showed that two deep levels were commonly observed, one slightly below midgap, 1/2 Eg (D_1) and one at 3/4 Eg (D_2). The near midgap center D_1, in bulk grown p-type $Hg_{1-x}Cd_xTe$ has a density proportional to V_{Hg}^{--} vacancy concentration.

Another proposed scheme associated with cation vacancy in HgCdTe developed from the admittance data has been previously reported by Kinch.[54] He proposed an alternative explanation involving two levels; 15 and 60 meV. The level of 60 meV was designated as a doubly ionized level V_{Hg}^{--}, with the shallower level as V_{Hg}^{-} at ~ 15 meV. The trapping level measurements which are reported here provide additional evidence that LPE HgCdTe material has similar defects observed in bulk HgCdTe reported by Kinch.

This Section reports on the admittance measurements on two $Hg_{1-x}Cd_xTe$ diodes fabricated on p-type LPE HgCdTe epilayers. The LPE layers on which these devices were grown had roughly the same bandgap. Sample A (4-31) had Eg = 268 meV while sample B (3-524) had Eg = 252 meV. The material was as-grown p-type in both cases with peak hole concentrations approximately 10^{16} cm^{-3} as

determined by a standard Van der Pauw technique. The 77K Hall data on these epilayers are summarized in Table 4 with the results of our experiment. n^+/p junctions were formed by boron ion implantation. The test diodes showed a cutoff wavelength of 4.6 μm at 77K and the R_0A product of a representative device was 1×10^4 - 10^6 Ω-cm^2 at 77K.

Table 4
Electrical Properties Measured at 77K and Hole Trap Levels
Obtained with Admittance and Hall Measurements

Sample	Electrical Properties of p-type $Hg_{1-x}Cd_xTe$		E_1 (meV)	E_2 (meV)
A (4-31)	Eg	0.268 eV	23	70
	Hole conc	6×10^{16} cm^{-3}		
	Hole mobility	278 cm^2/V-s		
B (3-524)	Eg	0.252 eV	13	40
	Hole conc	2×10^{16} cm^{-3}		
	Hole mobility	231 cm^2/V-s		
			13.2 (Hall meas.)	

The predominant background impurities in LPE $Hg_{1-x}Cd_xTe$ determined by SSMS were Al, Si, Fe and Se in the order of ~ 1 ppm. Light metal impurities (Li, Na, K and Ga) were determined by SIMS. AES analysis of as-grown surfaces of LPE HgCdTe show an appreciable amount of contaminants (S, O, C, Cl) only up to 30A deep and the surface contaminants were not detectable beyond 100A deep in LPE HgCdTe.

Atomic absorption (AA) analysis indicated Fe element typically 0.2 - 1.5 ppm. Temperature dependent Hall measurements show the presence of a level at 15 ± 5 meV from the valence band in similar Cd composition x of LPE $Hg_{1-x}Cd_xTe$ epilayers.

Figure 31 shows the characteristic admittance spectrum obtained from sample B as a function of temperature operating at 1 MHz. The admittance spectrum for this sample A shows the presence of two majority carrier (hole) traps. The energy of these traps is determined by measuring the peak position vs temperature for different driving frequencies. An Arrhenius plot of this data yields the energy as the slope shown in Fig. 32. Sample A shows the similar admittance data as sample B. However, temperature dependence of the shallower level peaks in the two samples yield the two different levels; 13 meV for the hole trap in sample 3-524 and an energy of 23 meV for the trap in sample 4-31. The difference in energy is outside experimental error in the measurement which is typically 10% and thus it is likely that the traps are associated with two different defects or may be related to background defect concentration which will be discussed in detail later.

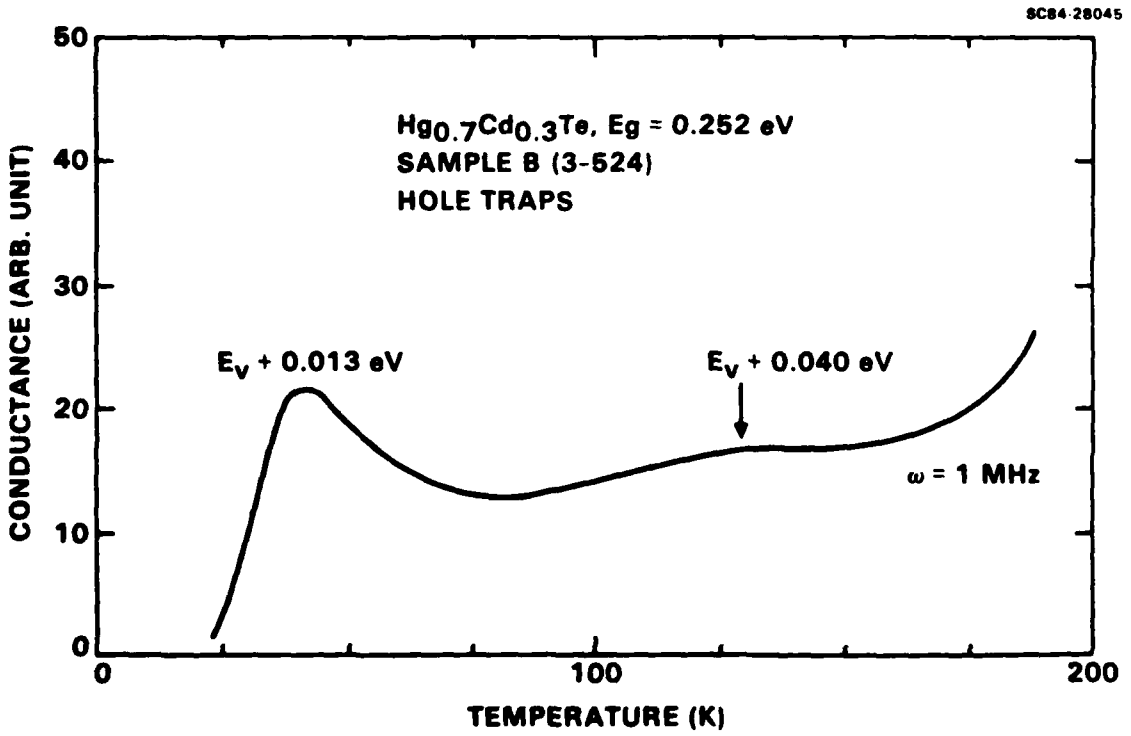

Fig. 31 Admittance spectrum on an n^+-p photodiode fabricated on LPE $Hg_{0.7}Cd_{0.3}Te$.

SC5305.6FR

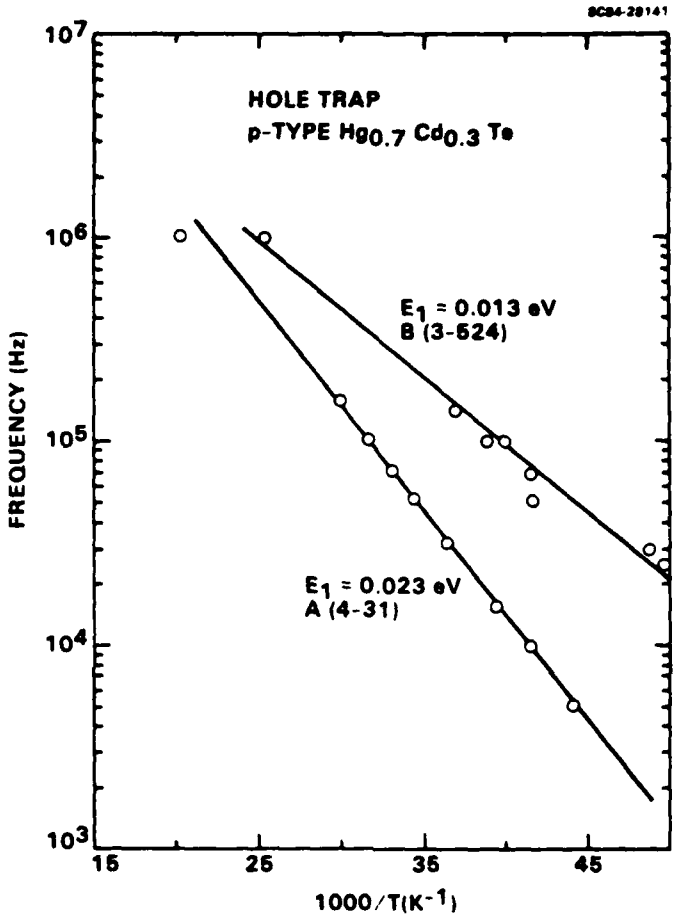

Fig. 32 Frequency dependence of admttance measurements of n^+-p diodes as a function of temperature.

It was not possible to obtain data for an Arrhenius plot from the higher energy traps because the width of the peak was too broad. However, an energy can be obtained if one assumes that the traps all have similar capture cross sections for majority carriers. In this case we estimate an energy of 40 meV for the deeper level in 3-524 and 70 meV for the deeper level in 4-31. It is interesting to note that the spectra are very similar in both samples and that the ratio between energies of the levels is roughly 3 in both cases.

The similarities between the admittance spectra suggest that there may be a correlation between the shallower and deeper levels. It is interesting to consider the possibility that the level is associated with a double acceptor. In such a case the low energy level would be associated with the first ionization of the defect and the deeper level with the second ionization of the defect. Possible candidate for such defects are substitutional C_{Te} and Si_{Te} both of which are expected to be double acceptors[55] and which often occur as impurities.

Hall measurements were made on sample B to verify the ionization energies of the acceptor in $Hg_{0.7}Cd_{0.3}Te$. The Hall effect was measured in a standard Van der Pauw technique by using a magnetic field of 6 KG for the temperature dependence measurements. The temperature dependence of hole concentration for sample B is shown in Fig. 33. The acceptor ionization energy obtained for sample B was 13 meV, which provide confirming evidence of the shallower level obtained by admittance measurements on the same sample. However, sample B shows only a shallow level 13 meV, but it did not show any deeper level. The 13 meV acceptor has been previously observed by Scott, Stelzer and Hager.[52] Furthermore, they also reported that the ionization energy changes depending upon a hole concentration. In order to investigate the dependence of hole concentration on the ionization energy, a Hg-annealing study was carried out on a similar sample from a different LPE run as a function temperature to change hole concentrations as shown in Fig. 34. Our result shows that the shallow energy level varies from 10 meV with $p \simeq 5.9 \times 10^{15}$ cm^{-3} to 20 meV with $p \simeq 1.0 \times 10^{17}$ cm^{-3}.

The increase in the acceptor ionization energy with hole concentrations (N_A) suggest that the 13 meV acceptor level may be associated with Hg vacancy or that the main contribution to the acceptor energy changes may be correlated with a vacancy related impurity-vacancy complex. These observations suggest that at least qualitatively the shallow level (e.g., 13 meV for sample B) is mainly due to an intrinsic defect controlled by the native defect of Hg vacancy rather than an extrinsic defect controlled by impurity because its energy level increases with acceptor carrier concentration as shown in

SC5305.6FR

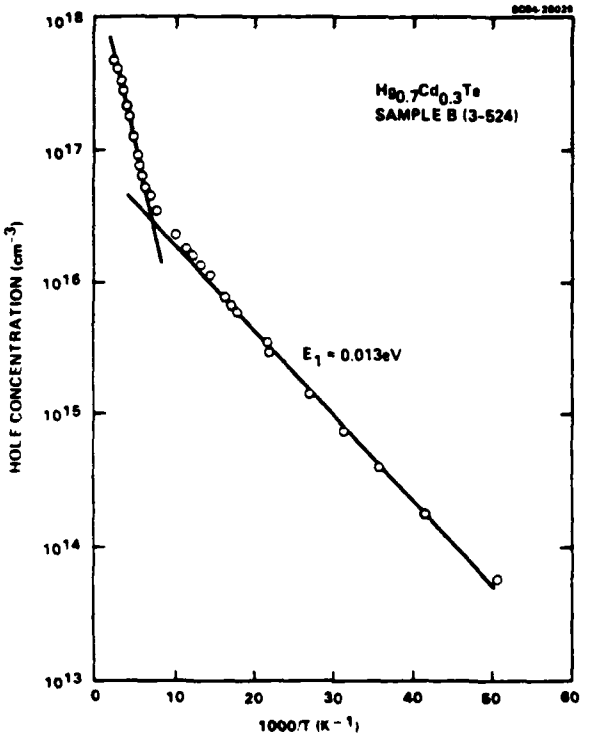

Fig. 33 Hall effect measurement obtained on $Hg_{0.7}Cd_{0.3}Te$ sample. An activation energy obtained from low temperature data is 13 meV for sample 3-524.

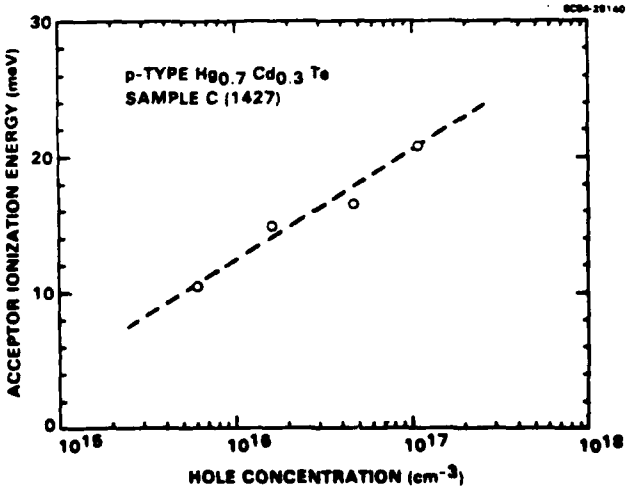

Fig. 34 Dependence of acceptor ionization energies on hole concentration. The data were obtained from Hall effect measurements as a function of temperature on four samples with different background hole carrier concentration.

Fig. 34. Since the deeper level (e.g., 40 meV for sample B) could not be examined by similar Hall effect measurements, it is not possible to tell whether these deep levels observed are also related to native vacancy defects. For these reasons it is useful to compare the E_1 value and hole concentrations of 4-31 to those measured in 1427 sample. Note deeper E_1 value may be related to higher hole concentration in 4-31 consistant with 1427 measurements. This observation suggests that association of two singly ionized vacancies perhaps near dislocation may give higher ionization energies. The nature of the deeper level is not clear. However, it seems plausible that these deeper levels are associated with second ionization energy of the shallow defect. Then the shallow level and the deeper level may be related to the first and second ionization energy of a Hg vacancy in HgCdTe.

The second possibility, that the level is associated with a double acceptor, is related to the group IV impurities. For example, substitutional C_{Te} and Si_{Te} are expected to be double acceptors and these impurities often occur as common impurities in HgCdTe. However, it is unlikely in layers grown at low T from Te solution. Another possibility, reported by Hunter and McGill[35] on luminescence studies, indicated that the presence of a shallow acceptor level at $E_v \pm 0.015$ eV seems to be due to gold (Au) on the cation sites. Thus, we cannot rule out substitutional Au_{Hg} in cation sites. More detailed electronic properties for Au-doped HgCdTe ($x = 0.48$) have been obtained by Meilainen and Jones[56] using deep level transient spectroscopy (DLTS). Two deep levels were observed; each had energy levels between E_v + 1/4 Eg and E_v + 1/2 Eg. The deep level at the near midgap level was also observed in undoped HgCdTe and a new level was found in the lower half of the bandgap.

In summary, we have made admittance measurements on p-type LPE $Hg_{0.7}Cd_{0.3}Te$. The two hole trap levels in one sample were 13 and 40 meV, and 23 and 70 meV for the other sample. Hall measurements were used to verify the lowest energy level of the acceptor. We also noted increases in the lower energy level from 10 to 20 meV with hole carrier concentrations from 6×10^{15} to 1×10^{17} cm^{-3}.

9.0 CONCLUSIONS AND RECOMMENDATIONS

9.1 Conclusions

The purpose of this three year program was to study the basic physics of defects in CdTe and HgCdTe material. In order to improve the fundamental understanding of the defect properties in HgCdTe, four basic areas were focused upon: (1) study of vacancy formation in $Hg_{1-x}Cd_xTe$; (2) electrical and metallurgical study of defects; (3) optical study of defects and impurities; and (4) study of the electrical properties of the implanted junction using an n^+-p photodiode structure.

The major conclusions of this work are the following:

1. The cation vacancy formation energy (E_f) of $Hg_{1-x}Cd_xTe$ is found to be E = 0.9 ± 0.1 eV. Within experimental error, this value is also found to be independent of the composition x of the alloys that were tried (x = 0.21, 0.3 and 0.43). The vacancies are predominantly charged at 77K and are predominantly in a doubly ionized state at both the annealing temperature and 77K.

2. We have examined the electrical transport properties of both as-grown p-type and Hg-annealed n-type LPE $Hg_{1-x}Cd_xTe$ epilayers. Our measurements show that the transport properties of LPE $Hg_{1-x}Cd_xTe$ are comparable to the best bulk $Hg_{1-x}Cd_xTe$.

3. The nature of Te precipitates in CdTe has been identified by Auger, x-ray diffraction and micro-Raman spectroscopy. The x-ray result shows that the precipitated Te in Bridgman grown CdTe crystals has the same structural phase as observed in elemental Te under high pressure.

4. The noble gases were incorporated into the cation vacancy in $Hg_{1-x}Cd_xTe$ and the defect-impurity equilibrium studied. Characteristic features observed are reduced hole carrier concentrtion and higher mobilities.

5. From the temperature dependence of both the integrated photoluminescence (PL) intensity and the peak position of LPE $Hg_{1-x}Cd_xTe$ and CdTe substrates, it is established that the two PL lines are related and could both be bound exciton recombination from the same neutral donor.

6. Far infrared absorption spectral of Cu-doped CdTe exhibit an unique feature of the Cu impurity modes: (1) several sets of sharp transitions, each set separated by 171 cm^{-1} (LO phonon energy); (2) each set consists of three sharp lines each separated by 30 cm^{-1}, which we believe corresponds to TA phonon energies occurring at the x-point.

7. Admittance spectra for p-type MWIR $Hg_{1-x}Cd_xTe$ ($x = 0.3$) show the presence of two majority carrier (hole) traps. The hole trap levels in one sample were 13 and 40 meV, and 23 and 70 meV for a second sample. Hall measurements were used to verify the lowest energy level of the acceptor. Dependence of the acceptor ionization energy on hole concentration suggests that the shallow level is associated with native defects controlled by Hg vacancies rather than impuritites.

9.2 Recommendations

It became clear during this defect study that accurate values of the zone center optical phonon frequencies of CdTe were not available in the literature. Continued study of both bulk and defect properties of CdTe and HgCdTe is important to shed light on the improvement of our further under-

standing in material and device physics. We believe that the ground work has been established for careful and systematic studies.

1. Low temperature infrared absorption studies on Xe (or other noble gas) doped HgCdTe could help to clarify the identity of the intrinsic defects.

2. Continued study of photoluminescence combined with far infrared absorption measurements on intentionally doped CdTe may provide insight into defect formation and identifications to isolate the residual impurities in nominally undoped CdTe and HgCdTe samples.

3. The most convincing way to establish the relationship between A and B lines (see Section 5.0) would be to measure the photoluminescence spectra of various alloys between CdTe and $Hg_{1-x}Cd_xTe$ and plot the activation energy as a function of x.

10.0 REFERENCES

1. C.C. Wang, S.H. Shin, M. Chu, M. Lanir, A.H.B. Vanderwyck, J. Electrochem. Soc. 127, 175 (1980).

2. S.H. Shin, M. Chu, A.H.B. Vanderwyck, M. Lanir and C.C. Wang, J. Appl. Phys. 51(7), 3772 (1980).

3. J.L. Schmit, J. Appl. Phys. 41, 2876 (1970).

4. G. Bastard, Proceedings of the Third International Conference on the Physics of Narrow Gap Semiconductor, Warsaw 1977 (PWN-Polish Scientific, Warszawa, 1978).

5. R. Dornhaus and G. Nimtz, Solid State Physics, (Springer, Berlin 1976).

6. M.A. Kinch, M.J. Brau and A. Simmons, J. Appl. Phys. 44, 1649 (1973).

7. W. Scott, J. Appl. Phys. 43, 1055 (1972).

8. J.H. Dubowski, T. Dietl, W. Szymanska and R.R. Galazka, J. Phys. Chem. Solids 42, 351 (1981).

9. R.D. Graft, F.F. Carlson, J.H. Dinan, P.R. Boyd and R.E. Longshore, J. Vac. Sci. Technol A.

10. Y. Nemirovsky and E. Finkman, J. Appl. Phys. 50, 8107 (1979).

11. G.L. Hansen and J.L. Schmit and T.N. Casselman, J. Appl. Phys. 53, 7099 (1982); G.L. Hansen and J.L. Schmidt, ibid 54, 1639 (1983).

12. I.M. Baker, F.A. Capocci, D.E. Charlton and J.T.M. Wotherspoon, Sol. St. Elect. 21, 1475 (1978).

13. C. Morgan-Pond and R. Raghavan, Phys. Rev. accepted.

14. 2. H.R. Vydyanath, J. Electrochem. Soc. 128, 2609 (1981), and H.R. Vydyanath, J.C. Donovan and D.A. Nelson, J. Electrochem. Soc. 128, 2625 (1981).

15. J.L. Schmit and E.L. Stelzer, J. Electron. Mater. 7, 65 (1978).

16. K.C. Dimiduk, W.G. Opyd, J.F. Gibbons, T.W. Sigmon, T.J. Magee and R.D. Ormond, J. Vac. Sci. Technol. A1(3), 1661 (1983).

17. A-B. Chen, A. Sher and W.E. Spicer, J. Vac. Sci. Technol. A1(3), 1674 (1983).

18. C.H. Su, P.K. Liao and R.F. Brebrick, J. Electron. Mater. 12(5), 771 (1983).

19. F.A. Kroger, The Chemistry of Imperfect Crystals, second revised edition 2, North Holland (1974).

20. J.A. Van Vechten, Ch. 1 in Vol. 3, Handbook on Semiconductors, T.S. Moss, ed., (New York: North-Holland, 1980).

21. C.E. Jones, private communication.

22. J.C. Jamieson and D.B. McWhan, J. Chem. Phys. 43, 1140 (1965).

23. F. Adar, R. Chin and S.H. Shin (unpublished).

24. G. Lucovsky, R.C. Keezer and Bristein, Sol. State Comm. 5, 439 (1967).

25. W. Richter, J.B. Renucci and M. Cardona, Phys. State Sol. 56(b), 233 (1973).

26. P.J. Dean, B.J. Fitzpatrick and R.N. Bhargava , Phys. Rev. B26, 2016 (1982).

27. R.N. Bhargava, J. Cryst. Growth 59, 15 (1982).

28. C.L. Jones, M.J.T. Quelch, P. Copper and J.J. Gosney, J. Appl. Phys. 53(12), 9080 (1982).

29. S.H. Shin, M. Khoshnevisan, C. Morgan-Pond and R. Raghavan (to be published).

30. N. Burger, K. Thonke, R. Sauer and G. Pensl, Phys. Rev. Lett. 52, 1645 (1984).

31. K.R. Zanio, "Semiconductor and Semimetals," edited by R.K. Willardson and A.C. Beer (Adademic Press, NY, 13, 1978).

32. C.T. Elliott, I Melngailes, T.C. Harman and A.G. Foyt, J. Phys. Chem Solids, 33, 1527 (1972).

33. V.I. Ivanov-Omskii, V.A. Maltseva, A.D. Britov and S.D. Sivachenko, Phys. Status Solidi A 46, 77 (1978).

34. M.G. Andrukhiv, V.A. Maltseva, V.I. Ivanov-Omskii, V.K. Ogorodnikov and T. Ts. Titievo, Fiz. Tekh. Poluprovodn 13, 362 (1979) (Sov. Phys. Semocond. 13, 210 (1979)).

35. A.T. Hunter and T.C. McGill, J. Appl. Phys. 52, 5779 (1981); J. Vac. Sci. Technol. 21, 205 (1982).

36. R.E. Halsted, in Physics and Chemistry of II-IV Compounds, ed. by M. Aven and J.S. Prener (North-Holland, Amsterdam, 417, 1967).

37. D. Bensahel, J. Phys. (Paris) 40, 1062 (1979).

38. T. Taguchi, J. Shirafuju and Y. Inuishi, Inst. Phys. Conf. Ser. 31, 426 (1977).

39. C.B. Norris and K.R. Zanio, J. Appl. Phys. 53, 6347 (1982).

40. P. Hiesinger, S. Suga, F. Wilman and W. Dreybrodt, Phys. Status Solidi B 67, 641 (1975).

41. T.J. McGee and G.R. Woolhouse, "Extended Abstracts of the 1983 U.S. Workshop on the Physics and Chemistry of Mercury Cadmium Telluride," Dallas, 71, February 1983.

42. R. Dornhaus and G. Nimtz, Springer Tracks in Modern Physics, Solid State Physics, ed by G. Hohler (Springer, Berlin 1976), 78, 93.

43. J.L. Schmit, J. Appl. Phys. 41, 2876 (1970).

44. M.W. Scott, J. Appl. Phys. 40, 40787 (1969).

45. C.G. Osbourn and D.L. Smith, Phys. Rev. B 20, 1556 (1979).

46. E. Molva, J.P. Chamonal, G. Milchberg, K. Saminadayar, B. Pajot and G. Neu, Sol. State Commun. 44, 351 (1982).

47. B. Furgolle, M. Hoclet, M. Vandevyver, Y. Marfaing and R. Triboulet, Sol. State Commun. 14, 1237 (1974).

48. D.N. Talwar and M. Vandevyver, J. Appl. Phys. 56(b), 1601 (1984).

49. O.M. Stafsudd, F.A. Haak and K. Radisavjevic, J. Opt. Soc. of Am. 57, 1475 (1967).

50. G.A. Slack, F.S. Ham and R.M. Chrenko, Phys. Rev. 152, 376 (1966).

51. A. Moordian and T.C. Harman, Proc. of Conf. on the Physics of Semimetals and Narrow Gap Semiconductors, 297 (1971).

52. W. Scott, E.L. Stelzer and R.J. Hager, J. Appl. Phys. 47, 1408 (1976).

53. D.O. Polla, W. Scott and C.E. Jones, Proc. Intl. Conf. on Phys. of Narrow-Gap Sem. p. 123 (1981), Linz, Austria.

54. M.A. Kinch, J. Vac. Sci. Technol. 21(1), 215 (1982).

55. C.A. Merilainen and C.E. Jones, J. Vac. Sci. Technol. A1(3), 1637 (1983).

APPENDIX

I. ELECTRICAL PROPERTIES OF AS-GROWN $Hg_{1-x}Cd_xTe$ EPITAXIAL LAYERS

Electrical properties of as-grown $Hg_{1-x}Cd_xTe$ epitaxial layers

S. H. Shin, M. Chu, A. H. B. Vanderwyck, M. Lanir, and C. C. Wang
Rockwell International Science Center, Thousand Oaks, California 91360

(Received 6 December 1979; accepted for publication 5 March 1980)

The Hall coefficient and resistivity of $Hg_{1-x}Cd_xTe$ epitaxial layers with $0.195 < x < 0.351$, have been measured between 4 and 300 K. At 77 K the results for $x = 0.30$ show that as-grown epitaxial layers are p type, with a carrier concentration and mobility on the order of 1.2×10^{16} cm^{-3} and 400 cm^2/V s, respectively. The acceptor ionization energy determined by the Hall measurements is found to change with the energy gap of $Hg_{1-x}Cd_xTe$. The electrical parameters and compositional uniformity ($\Delta x = \pm 0.001$) of the epilayer for $x = 0.30$ indicate that the material is comparable to the best reported bulk $Hg_{1-x}Cd_xTe$ single crystal.

PACS numbers: 72.40. + w, 85.60.Gz, 85.30.De, 68.55. + b

I. INTRODUCTION

Recent interest in photovoltaic infrared detector in the 3–5-μm and 8–12-μm region has prompted a search for new techniques to grow large area and uniform $Hg_{1-x}Cd_xTe$ material. The availability of such material would allow new concepts for devices with higher quantum efficiency and operating temperature than the present extrinsic Si devices, and greater suitability for hybrid or monolithic focal planes than PbSnTe devices.

Recently, $Hg_{1-x}Cd_xTe$ epitaxial layers on CdTe substrates have been grown by liquid phase epitaxy by several groups.[1-4] Details of our work in growing uniform $Hg_{1-x}Cd_xTe$ epitaxial layers on CdTe (111) substrates are reported in Ref. 4. Furthermore, the excellent photodiode performance of devices[5] fabricated on epitaxial material have demonstrated that as-grown epitaxial layers are comparable to the best reported bulk $Hg_{1-x}Cd_xTe$ single crystals.

Electrical transport measurements on bulk p-type $Hg_{1-x}Cd_xTe$ have been reported.[6] Recently, Scott *et al.*[7] reported electrical and far-infrared optical properties of p-type $Hg_{1-x}Cd_xTe$ with x in the range 0.26–0.6; the highest Hall mobility was about 400 cm^2/V s at 50 K and carrier concentrations were from 4×10^{15} to 1×10^{17} cm^{-3}. More recently, Bratt *et al.*[8] reported electrical measurements on p- and n-type HgCdTe material grown by the solid-state recrystallization method; they obtained $N_A - N_D$ values from 6.5×10^{14} to 3.1×10^{15} and hole mobilities of about 600 cm^2/V s at 35 K for a composition of $x = 0.28$.

This paper reports on the electrical properties of p-type $Hg_{1-x}Cd_xTe$ epilayers, with emphasis on crystals of higher uniformity than have previously been achieved. State-of-the-art uniform layers of $Hg_{1-x}Cd_xTe$ were grown by liquid phase epitaxy on semi-insulating (111)A CdTe substrates. Variation in composition for $x = 0.307$ material was ± 0.001 over an area of 2.0×1.5 cm. The as-grown layers

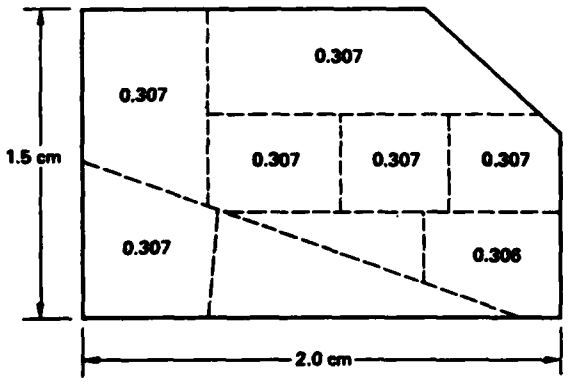

FIG. 1. Schematic diagram of compositional variation of $Hg_{1-x}Cd_xTe$ ($x = 0.307$) epilayer.

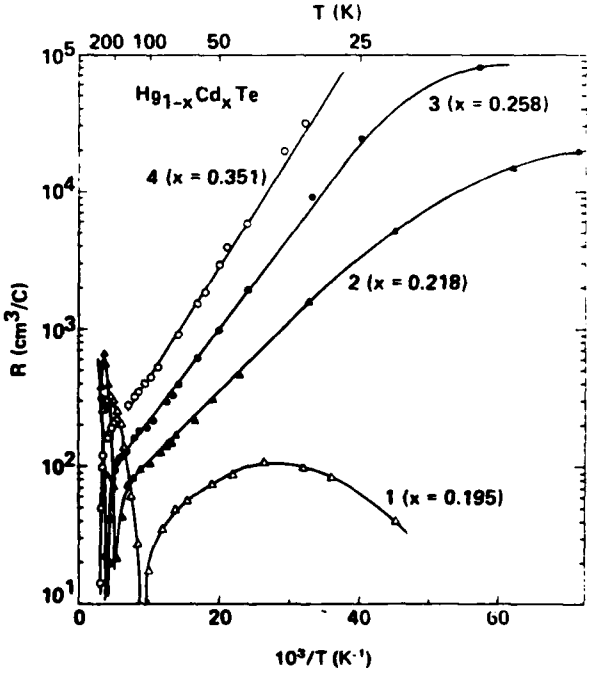

FIG. 2. Hall coefficients as function of reciprocal temperature. The numbers in parentheses indicate the alloy composition.

 0021-8979/80/073772-04$01.10

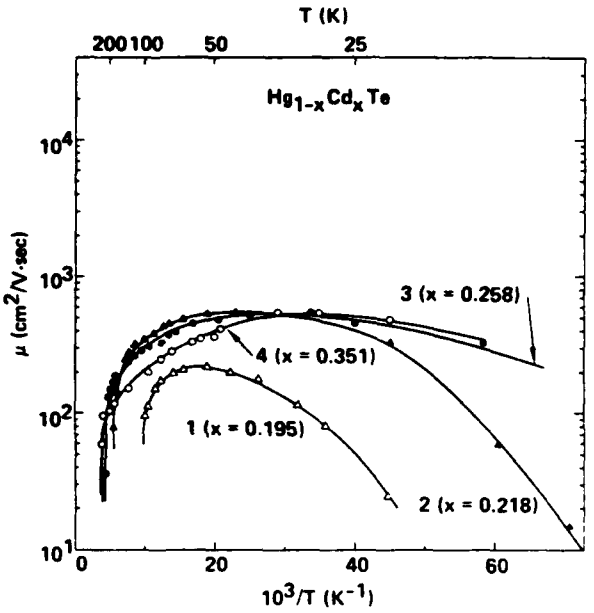

FIG. 3. Hall mobilities as function of temperature. The numbers in parentheses indicate the alloy composition.

exhibit hole carrier concentration and mobility on the order of 1.2×10^{16} cm^{-3} and about 400 cm^2/V s, respectively. The dependence of carrier concentration, Hall mobility, and acceptor ionization energy on Cd composition x is presented. To the best of our knowledge, no prior work has been reported on transport characterization of $Hg_{1-x}Cd_xTe$ epilayers grown on CdTe substrates.

II. EXPERIMENTAL RESULTS

A vertical furnace containing high-pressure Ar gas and a quartz tube was used for the growth of $Hg_{1-x}Cd_xTe$ epilayers on semi-insulating (111)A CdTe substrates. A Te-rich solution of HgCdTe was employed for the LPE growth. The source materials, Hg, CdTe, and excess Te metal, were loaded into the quartz tube in the furnace. After the source materials were reacted 650–700 °C for 60 min, the melt was cooled to the saturation temperature, approximately 500–550 °C. The growth time was adjusted to produce layers with thickness in the range 10–15 μm for all compositions. The quantities of Hg and CdTe in the melt were experimentally adjusted to achieve the required composition. Details of substrate preparation and growth process have been described in an earlier publication.[4]

Infrared transmission measurements at room temperature and cutoff wavelengths of photodiode spectral response at 77 K were used in determining the composition of grown layers. The compositional uniformity was established from the spectral response of measurements on arrays of detectors fabricated on different sections of the layer.

Figure 1 shows the compositional uniformity of an epilayer which was processd for fabricating detector arrays; variations in the composition and average value of the cutoff wavelength from each mosaic device are shown. In this layer, the total compositional variation in x was $\pm 1\times10^{-3}$ over an area 2×1.5 cm and was better than $\pm 3.0\times10^{-4}$ over a 1×0.3-cm area. This uniformity is significant for mosaic performance where the levels of both thermal and background noise are strongly band-gap dependent.

Hall coefficients R_H and resistivity in the temperature range from 4.5–300 K were measured by using the Van der Pauw technique with a magnetic field up to 6.3 kG. Since the substrates were semi-insulating, the Van der Pauw measurements provided unambiguous results of electrical parameters. The temperature dependence of the Hall coefficient for four representative $Hg_{1-x}Cd_xTe$ samples is shown in Fig. 2. Samples used in the investigation had values of $(N_A - N_D) = 2.8\times10^{16}$–$1.2\times10^{17}$ cm^{-3}, which were obtained from $(qR_H)^{-1}$, at the exhaustion region of the R_H vs $1/T$ curves, and Hall mobilities of 200–500 cm^2/V s at 77 K. In all cases, the Hall coefficient was negative at room temperature, because carrier transport is dominated by the intrinsic conduction. As temperature decreased, the mixed conduction occurring at around 100–200 K was common to all the samples. In the low-temperature region the slope of the curves of R_H vs $1/T$ increased with increasing energy gap. These results are similar to the earlier work on bulk crystals of Scott *et al.*[7] and Bratt *et al.*[8] It is noted that inversion temperatures were distinctly shifted to higher temperatures with increasing x. Carrier concentrations of these samples at 77 K were low, $\sim10^{16}$ cm^{-3}. In all cases, carrier freeze-out was observed and the Hall coefficient showed a reversal of sign at approximately 100–230 K, depending on Cd compositions.

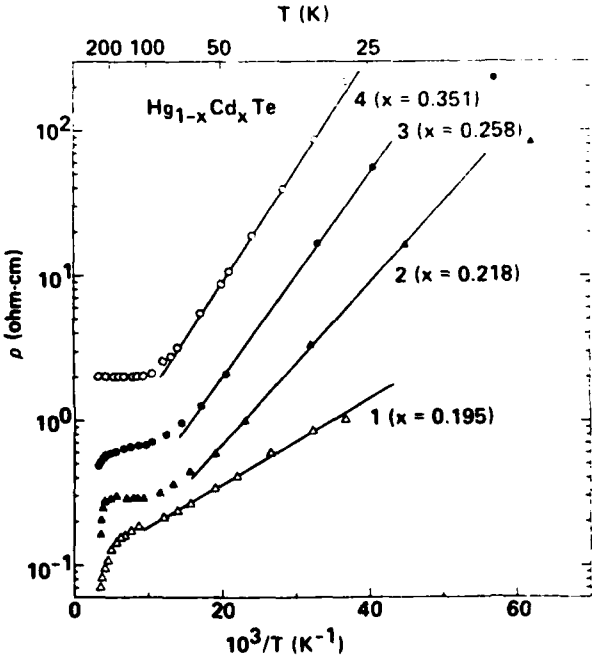

FIG. 4. Resistivity as function of temperature. The parentheses indicate the alloy composition.

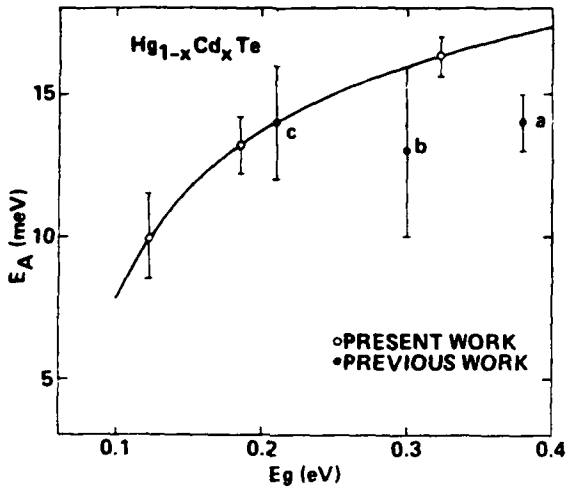

FIG. 5. Acceptor ionization energy E_A vs energy gap E_g for $Hg_{1-x}Cd_xTe$. The previous results are (a) Ref. 7, (b) Ref. 9, (c) Ref. 10.

Temperature dependence of the Hall mobility for the above samples is shown in Fig. 3. The Hall mobility of epilayers exhibited a region of intrinsic behavior in that it decreased rapidly with increasing temperatures. The mobility at lower temperatures also decreased with the temperature. This decrease is attributed to increasing impurity scattering.

The highest Hall mobility was about 550 cm^2/V s at about 40 K in samples for $x = 0.218 - 0.351$. In the other sample for $x = 0.195$, the mobility was about 210 cm^2/V s at 70 K.

Resistivity as a function of reciprocal temperature is shown in Fig. 4. It is clear that at lower temperatures, resistivity increased by two orders of magnitude compared to the room-temperature value in this discussed range of composition of $0.195 < x < 0.351$.

The acceptor ionization energy E_A shown in Fig. 5 was determined from the low-temperature Hall coefficient data. The values obtained were 6.4–16.3 meV for $Hg_{1-x}Cd_xTe$ in the range of $0.195 < x < 0.351$. However, the E_A value for sample 1 was not included in Fig. 5 because R vs $1/T$ data indicates an early onset of impurity band conduction and the straight-line portion is almost nonexistent. The results for the acceptor ionization energy are consistent with previous measurements[7,9,10] in the composition range $0.2 < x < 0.3$. Furthermore, the dependence of acceptor ionization energy on hole carrier concentration was found to be in excellent agreement with the data of Scott *et al.*[7] However, experimental values for the dependence of the acceptor ionization energy (E_A) on the band gap (E_g) are not available in the semiconductor region $0 \le Eg \le 1.6$ eV of the $Hg_{1-x}Cd_xTe$ alloy system.

III. DISCUSSION

For the analysis, we assume that as-grown p-type HgCdTe is partly compensated by donors, since the temperature dependence of the Hall mobilities in the interesting range of temperature is characteristic for compensated samples. For a partly compensated semiconductor, the temperature dependence of holes is described by[11]

$$p \propto \exp(E_A/kT),$$

where E_A is the acceptor ionization energy, k is Boltzman's constant, and T is the temperature. In Fig. 5, the ionization energies deduced from the temperature dependence of the Hall coefficients are given as function of the band gap E_g. Results of this analysis are summarized in Table I. It must be emphasized that the acceptor ionization energy estimated is strongly affected by the temperature dependence of E_g for the narrow gap semiconductor. Our results for acceptor ionization energy E_A in Fig. 5 are comparable to those of previous optical and transport measurements.[7,9,10]

The results of Fig. 4 show that the temperature dependence of the resistivity increased as x increased. This can be explained, at least somewhat quantitatively, by analyzing the position of the acceptor level when the composition x changes.

It is shown by Kharus and Shelushinia[12] that the dependence of E_A on E_g in the Hubbard model is governed by the density of states due to the shift of undeformed parabolic bands. Their calculations show that the acceptor ionization energy E_A rises by a factor of about 2 in the range of $0 < E_g < 250$ meV. In Fig. 5, our measured E_A is plotted as a function of the band gap. It is observed that the acceptor ionization energy E_A rises substantially with increasing E_g. We found that the increase in E_A is in a manner similar to the Hubbard model in Ref. 12.

However, the dependence of E_A on the band gap E_g is still open to question, because we do not as yet have a detailed model about the impurity states in $Hg_{1-x}Cd_xTe$.

IV. CONCLUSIONS

In summary, HgCdTe epilayers grown on CdTe substrates by liquid phase epitaxy show practically bulk-like carrier concentrations as well as mobilities. The experimental results on $Hg_{1-x}Cd_xTe$ epilayers are shown to be in good agreement with those measured on bulk materials. As-grown epitaxial $Hg_{1-x}Cd_xTe$ layers exhibit p-type conductivity with carrier concentrations 1.2×10^{16} cm^{-3} and a Hall mobility of about 400 cm^2/V s at 77 K. The electrical parameters and compositional uniformity of the epilayer over a 2×1.5-cm^2 area indicate that the material is comparable to the best reported bulk HgCdTe.

TABLE I. Electrical properties of as-grown $Hg_{1-x}Cd_xTe$.

Sample	X	$N_A - N_D$ (cm^{-3})	E_A (eV)
1	0.195	1.2×10^{17}	0.0064
2	0.218	5.6×10^{16}	0.0095
3	0.258	4.5×10^{16}	0.0132
4	0.351	2.8×10^{16}	0.0163

ACKNOWLEDGMENTS

We wish to thank M. Kim and W. E. Tennant for a number of stimulating conversations and D. T. Cheung, A. M. Andrews, and J. T. Longo for continuing support.

[1]M. Lanir, C. C. Wang, and A. H. B. Vanderwyck, Appl. Phys. Lett. **34**, 50 (1979).
[2]T. C. Harman, J. Electron. Mater. **8**, 191 (1979).
[3]J. L. Schmit and J. E. Bowers, Appl. Phys. Lett. **35**, 457 (1979).
[4]C. C. Wang, S. H. Shin, M. Chu, M. Lanir, and A. H. B. Vanderwyck, J. Electrochem. Soc. **127**, 175 (1980).
[5]C. C. Wang, M. Chu, S. H. Shin, W. E. Tennant, J. T. Cheung, M. Lanir, A. H. B. Vanderwyck, G. Williams, L. O. Bubulac, and R. Eisel, IEEE Trans. Electron. Devices (to be published); M. Lanir, S. H. Shin, A. H. B. Vanderwyck, L. O. Bubulac, R. Eisel, G. M. Williams, and W. E. Tennant, IEDM Digest, Washington, D.C., 1979; M. Chu, S. H. Shin, A. H. B. Vanderwyck, L. O. Bubulac, W. E. Tennant, and C. C. Wang, IEDM Digest, Washington, D.C., 1979.
[6]For a recent review, see R. Dornhous and J. Nimtz, *Solid State Physics* (*Springer Tracts in Modern Physics*; 78) (Springer-Verlag, Berlin, 1976).
[7]W. Scott, E. L. Stelzer, and R. J. Hager, J. Appl. Phys. **47**, 1408 (1976).
[8]P. R. Bratt, A. H. Lockwood, and K. J. Riley, Paper presented at IRIS Specialty Group Meeting on Infrared Detectors, Annapolis, Maryland, June 1978 (unpublished).
[9]C. T. Elliott, I. Melngailis, T. C. Harman, and A. G. Foyt, J. Phys. Chem. Solids **33**, 1527 (1972).
[10]R. Bichard, Y. Guedner, and P. Lavallard, Proceedings of the Third International Conference on the Physics of Narrow Gap Semiconductors, Warsaw (Poland), 1977 (unpublished).
[11]J. Blakemore, *Semiconductor Statistics* (Pergamon, New York, 1962).
[12]G. I. Kharus and N. G. Shelushinia, Sov. Phys. Semicond. **12** (3), 249 (1978).

END

FILMED

5-85

DTIC